

Twistophane Macrocycles with Integrated 6,6'-Connected-2,2'-Bipyridine Units: A New Lead Class of Fluorescence Sensors for Metal Ions

Paul N. W. Baxter*^[a]

Abstract: The new twistophane macrocycles **2** and **3** have been synthesised; these compounds are composed of a cyclically conjugated dehydrobenzoannulene framework that incorporates 6,6'-connected-2,2'-bipyridine moieties for the purpose of coordinating metal ions. The cyclophanes were characterised by spectroscopic techniques, and shown by molecular mechanics calculations to be helically twisted and chiral molecules that may exist in several possible ground state conformations. UV/vis spectroscopic studies revealed

that **2**, **3** and precursor **9** bind with different selectivities to particular members of the following small group of metal analytes: Cu^{II}, Ag^I, Hg^{II}, Tl^I and Pd^{II}. Significantly, **2**, **3** and **9** signal the presence of Cu^{II} ions through fluorescence emission quenching output responses. Furthermore, cyclophane **3** exhibited a particularly sensitive proton-

Keywords: alkynes · cyclooligomerization · cyclophanes · macrocyclic ligands · sensors

triggered chromogenic fluorescence response. With respect to their unique structural features, high analyte selectivity coupled with their enhanced and characteristic fluorescence emission responses, these molecules are among the first examples representing a new lead class of chemosensory materials. Compounds **2**, **3** and **9** and derivatives thereof may, therefore, be expected to find many future applications in the detection of metal-based environmental pollutants, biologically important trace elements and monitoring proton fluxes.

Introduction

Over the past 30 years, macrocyclic chemistry has developed into a field of major scientific and technological importance.^[1] Owing to their guest inclusion and complexation properties, a wealth of applications have been discovered for the vast range of macrocyclic structures thus far prepared. These applications include diverse areas such as: medical diagnostics and drug delivery,^[2a-d] analytical chemistry,^[3] metal extraction and separation,^[3, 4a-c] chemical synthesis,^[5] polymer chemistry,^[6] food science^[7] and, more recently, the domain of nanochemistry.^[8] They have also played a pivotal role in the synthesis and study of challenging molecular architecture and topology.^[9]

Of historic interest is the fact that one of the earliest reported macrocycle syntheses concerned the preparation of a

medium-sized ring that incorporated an ethyne group as an integral structural unit.^[10] However, interest in ethynyl-incorporated macrocycles remained dormant for nearly 50 years until the 1960's when annulenes became the target of synthetic effort,^[11] in order to determine whether molecules with expanded cyclic conjugation pathways obeyed the Hückel theory of aromaticity.^[12a-b] Interest in the field waned again until the early 1990's, at which point ethynyl macrocycles once again became the focus of intense research activity.^[13] The latter resurgence of interest was fuelled predominantly by the discovery of carbon buckyballs and nanotubes^[14] and the potential for the development of new classes of carbon allotropes, high carbon-content materials^[15a-g] and nanostructures.^[16]

Currently, cyclic ethynyl-containing materials collectively represent a significant proportion of all known macrocyclic architectures, encompassing a diverse variety of species such as annulenes,^[11, 12a-b, 17] dehydroannulenes,^[13, 18a-d] expanded radialenes,^[19a-b] $[n]$ pericyclines,^[13, 20a-b] $[n]$ rotanes, exploded $[n]$ rotanes^[13, 21a-b] and many types of ethynyl-incorporated cyclophanes.^[22a-c] Some of these materials exhibit intriguing properties such as liquid crystallinity^[23] and solid-state nanoporosity,^[24] and also can function as high-energy materials and as precursors to carbon nanotubules.^[13, 25]

In the light of the aforementioned considerations, a particularly interesting avenue of investigation would be to endow conjugated macrocycles of this type with sites for the

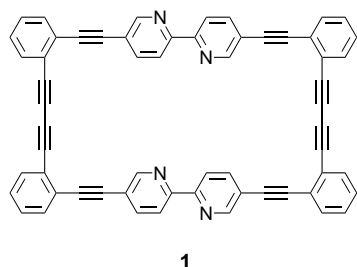
[a] Dr. P. N. W. Baxter

Laboratoire de Chimie Supramoléculaire
Institut Le Bel, Université Louis Pasteur
4 rue Blaise Pascal, 67000 Strasbourg (France)
Fax: (+33) 3-9024-1117
E-mail: pbaxter@chimie.u-strasbg.fr

Supporting information for this article is available on the WWW under <http://www.chemeurj.org> or from the author: Figures illustrating 1) the ¹H NMR spectroscopic variable temperature behaviour of **2**; 2) molecular models of the tubular conformation of **3**; 3) the UV/vis titration of **2** with successive amounts of Ag^I; and 4) the UV/vis titration of **3** with Ag^I.

purpose of binding metal ions.^[26a–c] A wealth of new functional physicochemical properties would be expected to emerge from such hybrid organic–inorganic materials, such as multiple redox, magnetic, photochemical, optical, catalytic, substrate inclusion, sensing ability and perhaps unusual mechanical behaviour.

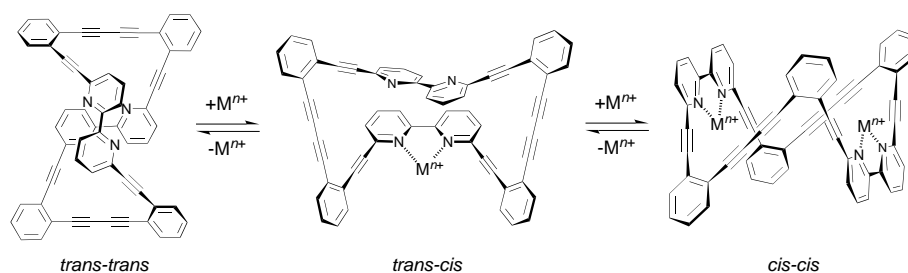
In previous work, preliminary investigations of this type were reported; these described the synthesis of a *ortho*-cyclically conjugated twistophane **1**.^[27a] Cyclophane **1** is



composed of a tetrabenzodehydroannulene-type hydrocarbon framework that incorporates two 5,5'-disubstituted-2,2'-bipyridine ligand units positioned on opposite sides of the macrocyclic ring.^[28a–g] It was anticipated that the highly conjugated structure of **1** would undergo significant electron-distribution perturbations upon coordination to metal ions of complementary size within the chelating ligand pocket. The electronic redistribution within **1** would in turn be translated into visual spectroscopic output signals with energies characteristic of particular metal ions. This in fact proved to be the case, and **1** was found to function as a specific chromogenic fluorescence sensor for Zn^{II} ions.^[27a]

For both of the bipyridine subunits of **1** to bind a single metal ion, the twisted hydrocarbon framework must slightly unwind, thereby allowing the bipyridine rings to rotate about their longitudinal axes and orient the four nitrogen lone pair electrons towards the interior of the macrocyclic cavity. Only a minimal change in the conformation of **1** is necessary for complete metal-ion coordination. In this case, the spectroscopic response resulting from a metal-ion binding event must originate principally from electron distribution perturbations relayed through the bipyridine nitrogen lone pairs.

However, a much greater perturbation in overall electron distribution would be expected to occur if the macrocycle was to additionally experience a significant change in conformation upon binding to a metal ion. In such a system, the metal-ion-triggered change in spatial geometry should result in an



Scheme 1. Expected conformational rearrangement of twistophane **2** upon sequential binding to metal ions.

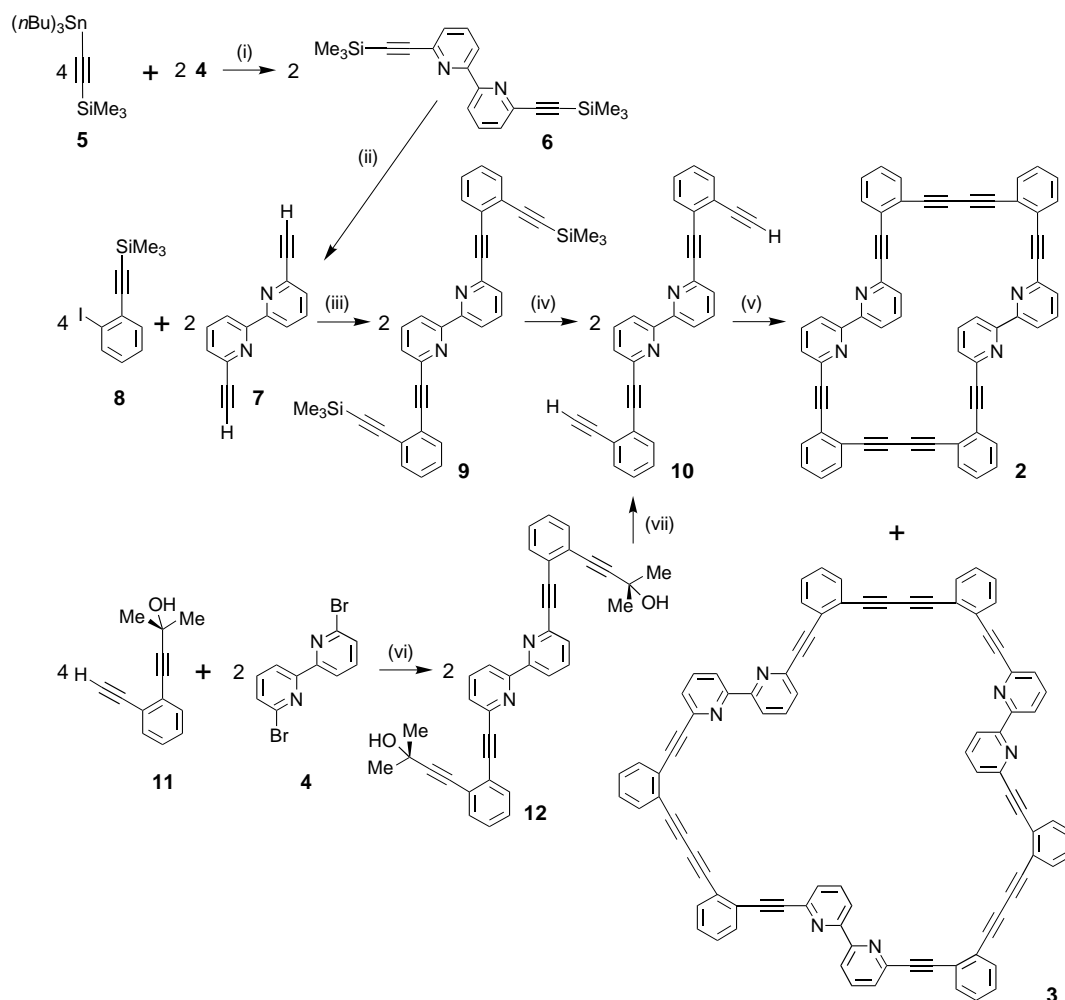
enhanced optical response and thus an amplified ion-sensory output signal.

Twistophane **2** is an isomeric analogue of **1** in which two 6,6'-disubstituted-2,2'-bipyridine units are incorporated into the tetrabenzodehydroannulene framework (Scheme 1). Molecular modelling studies on **2** revealed that it may potentially function as a mechano-responsive ion sensor that is capable of binding two metal ions, and in so doing, would be forced to undergo three consecutive changes in conformation (Scheme 1); while uncoordinated, **2** would reside in the conformation of lowest strain, in which the pyridine rings of each bipyridine unit are arranged in a *transoid* relationship (denoted *trans-trans* in Scheme 1). Upon coordination to the first metal ion, the twistophane **2** would have to partly unwind to allow one of the bipyridine units to adopt a *cisoid* conformation. The overall geometry would have to switch to a *trans-cis* arrangement as shown in Scheme 1. Binding of the second metal ion would force the remaining *transoid* bipyridine unit to convert to a *cisoid* conformation, thereby completely unwinding the macrocycle to give the geometrically open *cis-cis* cyclophane. Unlike its predecessor **1**, metal-ion binding to **2** would be accompanied by a dramatic change in overall geometry of the macrocyclic ring. As a result, the comparatively greater mechanically induced electronic perturbations may translate into an increased ion-sensing response for the latter cyclophane.^[29a–e]

The following full account describes the successful synthesis and characterisation of **2** and its trimeric analogue **3**, and a detailed spectroscopic investigation into the metal-ion sensing propensities of **2**, **3** and their precursor **9** (Scheme 2). The spectroscopic studies revealed that **2**, **3** and **9** exhibited different ion-binding properties, but all afforded characteristic and specific fluorescence quenching sensory outputs in the presence of Cu^{II} ions.^[30a–f]

Results and Discussion

Synthesis of **2 and **3**:** The macrocycles **2** and **3** were synthesised by two separate, six-step convergent pathways, each utilising the key building block 6,6'-dibromo-2,2'-bipyridine (**4**; Scheme 2; not all steps are shown). Thus the first synthetic approach started from the commercially available (2-bromophenylethynyl)trimethylsilane which was converted to the iodo derivative **8** by a lithiation/iodination protocol described previously.^[27a] The reaction between **8** and 6,6'-diethynyl-2,2'-bipyridine (**7**) under classical Sonogashira conditions by employing [PdCl₂(PPh₃)₂] and CuI as catalyst and cocatalyst, respectively, in a 1:1 mixture of toluene/Et₃N resulted in the formation of a disappointingly moderate yield (30%) of bipyridine **9**.^[31] Repetition of the reaction in a 6:1 mixture of pyridine/Et₃N gave only a slight increase in the yield of **9** to 35%. However, changing the reaction solvent to an 8:1 mixture of toluene/Et₃N



Scheme 2. Synthesis of macrocycles **2** and **3**. i) $[\text{Pd}(\text{PPh}_3)_4]$ cat., toluene, 122°C , 36 h (63%); ii) aq. $\text{KOH}/\text{MeOH}/\text{THF}$, 20°C , 20 h; iii) $[\text{PdCl}_2(\text{dppf})] \cdot \text{CH}_2\text{Cl}_2$ and CuI cat., toluene, Et_3N , 20°C , 8 d (86%); iv) $1\text{M } (n\text{Bu})_4\text{NF}$, THF , H_2O , 20°C , 18 h (97%); v) Hay procedure: CuCl cat., O_2 , pyridine, 20°C , 25 days, 13% (**2**); Breslow procedure: CuCl , $[\text{Cu}_2(\text{OAc})_4]$, 60°C , 6 h then 20°C for 14 days, 9% (**2**), 5% (**3**); vi) $[\text{PdCl}_2(\text{PPh}_3)_2]$, CuI cat., THF , Et_3N , 20°C , 7 d (51%); vii) KOH , toluene, 110°C , 7 h (79%).

and, most importantly, by using $[\text{PdCl}_2(\text{dppf})]$ as the catalyst resulted in a dramatic increase in the yield of **9** to 80–86%. The enhancement in catalyst activity in the case of $[\text{PdCl}_2(\text{dppf})]$ can be correlated with the unusual P-Pd-P bite angle, which lies at an optimum for facilitating both the oxidative addition of the aryl halide and reductive elimination steps in the catalytic cycle.^[32] To date, this catalyst has only rarely been used for effecting the Sonogashira mediated alkyne reactions of aryl halides. In the light of the above observation, a more widespread utility may be discovered for $[\text{PdCl}_2(\text{dppf})]$ in cases in which the conventional catalysts give low yields and in which sensitive substrates are employed.

Bipyridine **7**^[33a–c] was prepared in two steps from **4** via **6**. The Sonogashira reaction of **4** with trimethylsilyl ethyne has been reported to give **6** in 87% yield.^[33b–c] In the course of experimental investigations aimed at exploring the scope of the Pd-catalysed alkyne reactions of heterocycles with alkyne-stannanes, it was decided to investigate the possibility of using a Stille-type alkyne reaction for the preparation of **6**.^[34] Thus heating **4** with an excess of **5**, LiCl and $[\text{Pd}(\text{PPh}_3)_4]$ in toluene resulted in the successful generation of **6** in 63% isolated yield.

Having defined the optimal conditions for the preparation of **9**, it was then desilylated with TBAF in THF to give the macrocycle precursor **10**. The yield of this deprotection appeared to be particularly sensitive to the water content of the reaction solution. If **9** was deprotected in anhydrous or normal reagent grade THF, the reaction became dark brown, and only low yields of **10** were subsequently isolated. If, however, a few drops of water were added to the THF reaction solution prior to TBAF addition, the deprotection then proceeded normally with the formation of **10** in high yield. The fluoride ion in the commercial 1M TBAF may be acting as a strong nucleophile to initiate polymerisation-type reactions as well as the desired desilylation. The presence of excess water considerably reduces both the nucleophilicity and basicity of fluoride anions, presumably enabling the desilylation to occur alone.

In the second synthetic approach to **10**, commercial 1,2-diiodobenzene was converted to the monoprotected diethyne **11**,^[35] which reacted with **4** under Sonogashira conditions to provide the diprotected bipyridine **12** in a reasonable (51%) isolated yield. The yield of this transformation appeared to be highly dependent on the type of reaction

solvent, with much lower yields of **12** resulting if toluene was used in place of THF. Subsequent base-catalysed elimination of acetone from **12** afforded diethyne **10** in 79% yield.

With the precursor diethyne **10** in hand, the synthesis of the target macrocycle **2** could finally be undertaken. Initially, it was decided to prepare **2** by the oxidative cyclisation of **10** under medium dilution conditions by using the Hay coupling protocol,^[36] as this methodology has been successfully employed for the generation of **1** as reported previously.^[27a] However, this approach resulted in the isolation of a surprisingly low yield (13%) of the desired cyclophane **2** relative to that of **1** (34%) under similar conditions. The major reaction product by mass recovery consisted of a brown solid, totally insoluble in the common laboratory solvents. This material may be composed of uncyclised oligomers and polymers and possibly high molecular mass cyclooligomers.

An effective method of improving the poor yields often encountered during the copper-catalysed oxidative macrocyclisation of terminal alkynes has been reported by Breslow et al.^[37] In this procedure, a mixture of CuCl and [Cu₂(OAc)₄], both present in large excess relative to the alkyne substrate, were found to considerably improve the yield of a macrobicyclic compared to the use of each copper reagent alone. Also, these conditions do not require the reaction to be continually exposed to oxygen gas. Application of this modification to the cyclisation of **10** resulted in the formation of **2** in 9% yield, that is, lower than that of the Hay procedure! However, a small quantity of the trimer-cyclophane **3** was isolated from this reaction in 5% yield.

Although the exact factors responsible for the poor yield of **2** are currently unknown, negative ion-templating phenomena may account for one possible cause. The relatively enhanced yield of **1** is consistent with a positive ion-templating mechanism, in which the coordination of two bipyridine macrocycle precursors to the same Cu^{III} ion would orient the four terminal ethynes into the correct position for subsequent cyclisation to **1**. In the case of **2**, the above process would result in the formation of a coordinated macrocyclic structure that possesses significantly greater ring strain. The avoidance of ring strain may preferentially direct the reaction pathway toward the formation of linear oligomers and polymers. The copper ions may therefore be playing the role of a negative templating agent during the formation of **2**.^[22a–b]

Characterisation of cyclophanes 2 and 3: The structure of the products isolated from the copper-mediated Hay and Breslow couplings of **10** were established to be that of the macrocyclic architectures **2** and **3** (Scheme 2) on the basis of MS and IR, ¹H and ¹³C NMR spectroscopic studies.

The FAB mass spectra of the coupling products recorded in 10–20% CF₃COOH/CHCl₃ each displayed a single isotope cluster peak at an *m/z* of 805 and 1208; these correspond exactly to that calculated for the [M⁺+H] isotopic envelopes of macrocycles **2** and **3**, respectively. This structural assignment was further substantiated by high-resolution FAB mass spectroscopic measurements of the [M⁺+H] isotopic envelopes, which confirmed the exact elemental composition of the products to be C₆₀H₂₉N₄ and C₉₀H₄₃N₆ in accordance with

the macrocyclic structures **2** and **3**, respectively, plus one hydrogen in each case.

The infrared spectra of the coupling products of **10** were also supportive of the macrocyclic structural assignments of **2** and **3**, in that vibrational modes characteristic of the ν(H–C≡) stretch of terminal alkynes were completely absent in each case. This result establishes that the coupling products are in fact macrocyclic, and not linear oligomers with unreacted terminal ethyne groups.

The ¹³C NMR spectra of the coupling products of **10** each have fifteen peaks, consistent with the above macrocyclic structural assignments. The chemical shifts of four peaks corresponded to the chemically and magnetically inequivalent carbons of two unsymmetrically substituted alkyne groups, and the remaining eleven to inequivalent carbons of aromatic rings. In the case of **2**, it was possible to assign the proton-bearing C3, C4 and C5 pyridine-ring carbon atoms to the peaks at 120.6, 136.9 and 128.9 ppm respectively by an HMQC experiment.

The ¹H NMR spectra of both coupling products of **10**, also displayed the five sets of peaks (two of which overlapped) expected for the macrocyclic structures **2** and **3**. ¹H–¹H COSY measurements also verified that they were each single compounds and not mixtures of species. Peaks originating from the protons of terminal ethynes were completely absent in the spectra of both coupling products, lending further support for the macrocyclic identities of these compounds.

Spectral assignments were made on the basis of coupling constants, ¹H–¹H COSY correlations as well as comparisons with the spectra of **9**, **10** and **12**. Thus the multiplets at 7.44 and 7.41 ppm in **2** and **3**, respectively, were each assigned to the overlapping peaks of the phenyl H4 and H5 protons, and those at 7.66 and 7.65 ppm in **2** and **3**, respectively, were each assigned to the overlapping peaks of the phenyl H3 and H6 protons. The chemical shifts of the phenyl H3 proton appear to be quite sensitive to the substituent on the adjacent ethyne. In the case of **2** and **3** the phenyl H3 multiplet is observed further downfield relative to those of the precursors **9**, **10** and **12**, and overlaps with that of the phenyl H6 due to the similarity in electron-withdrawing ability of the phenylbutadiynyl and ethynylpyridyl groups (Figure 1). The characteristic doublet at approximately 8.1 ppm is the furthest downfield signal in the spectra of **2** and **3**, and corresponds to the pyridine H3 protons, which are anisotropically deshielded by the nitrogen lone-pair electrons of the adjacent pyridine ring. The remaining triplet and doublet at 7.74 and 7.61 ppm in **2** and at 7.35 and 7.47 ppm in **3** were, therefore, assigned to the pyridine H4 and H5 protons, respectively.

The chemical shifts of the H3 and H4 pyridine ring protons in **2** and all the pyridine ring protons in **3** are substantially shifted upfield in comparison to those of **9**, **10** and **12** (Figure 1). This evidence further establishes the macrocyclic identities of **2** and **3**, in that such shielding would be expected of protons pointing toward the interior of a macrocyclic cavity and/or lying alongside the face of an adjacent aromatic ring.

Molecular modelling and solution dynamics of 2 and 3: Information concerning the possible three-dimensional struc-

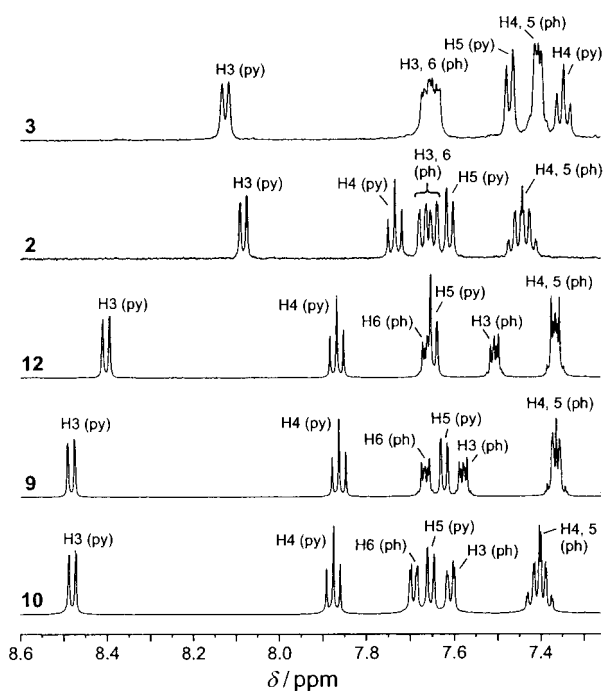


Figure 1. 500 MHz ^1H NMR spectra of **2**, **3**, **9**, **10** and **12** recorded in $\text{CDCl}_2\text{CDCl}_2$ at 20°C .

tures of **2** and **3** was obtained by AM1 semiempirical theoretical calculations.^[38] This study revealed that twistophane **2** could exist in three main conformations of similar energy (Figure 2). The conformers differ principally in the

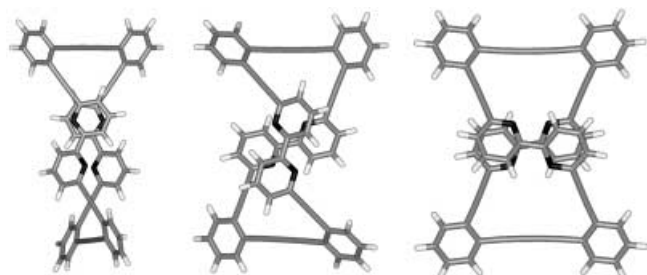


Figure 2. Energy-minimised structures of macrocycle **2**, showing the three principle conformations, denoted OO (left), PO (centre) and PP (right): plan view stick representation. Note that each conformer represents one of a pair of enantiomers. The minimisations were obtained by AM1 semiempirical calculations by using SPARTAN 02 Linux/Unix, Wavefunction, Irvine, CA (USA).

relative orientation of the two bipyridine subunits within each macrocyclic ring. Thus for each conformer, the longitudinal axes of the pair of bipyridines can be arranged both approximately parallel (denoted PP), both approximately orthogonal (denoted OO), or one approximately parallel and one orthogonal (denoted PO) to the axes of the butadiynes (Figure 2). Interestingly, all three conformers are hinged structures, as increasing the interpyridine dihedral angles within each bipyridine unit results in opening of the cyclophane to give a central box-shaped void. Lateral compression of the conformers, until each pair of bipyridine subunits are within van der Waals contact, results in a pronounced flexing

and bending of the butadiyne bridges. Each conformer is also helically twisted and chiral, and, therefore, can be represented as either one of a pair of enantiomers.

An inspection of CPK and wireframe models of **2** revealed that major distortions of the macrocyclic framework would be necessary in order to allow direct interconversion between enantiomers of the *same* conformer. The most sterically accessible mechanism for enantiomer interconversion of a given conformer must therefore proceed indirectly in several steps, which involve the sequential interconversion between enantiomers of *different* conformers. Interconversion between the three different conformers would require stepwise rotations of the bipyridine moieties about the mean axes through their ethyne substituents.

However, the ^1H NMR spectra of **2** and **9** in $\text{CDCl}_2\text{CDCl}_2$ solution change with variation in temperature in similar ways. The most pronounced shifts are experienced by the pyridine H3 protons, which move downfield by $\Delta\delta = 0.079$ ppm in **2** and 0.057 ppm in **9** upon increasing the temperature from 20 – 120°C . These downfield shifts reflect the increased rotational motion of the pyridine rings in **9** and indicate that **2** is at least flexible enough to allow changes in the dihedral angle between the bipyridine subunits of each bipyridine.^[39]

In the case of twistophane **3**, semiempirical AM1 calculations showed that this macrocycle was particularly conformationally mobile. The calculations revealed that **3** may potentially exist in a range of different collapsed and helically twisted conformations of similar energy, some of which possess interpyridine van der Waals contacts (Figure 3). An

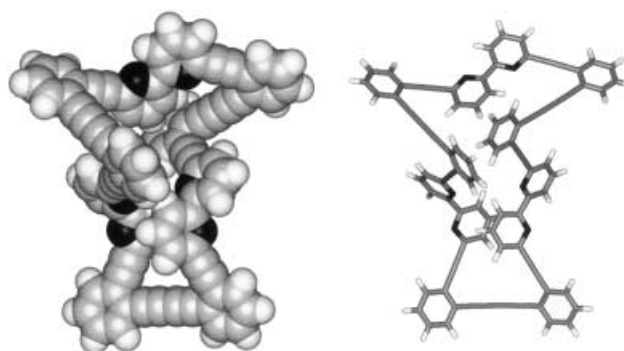


Figure 3. Energy-minimised structure of **3**, showing a collapsed and folded conformation: space-filling representation (left), stick representation (right). The minimisation was obtained by AM1 semiempirical calculations using SPARTAN 02 Linux/Unix.

inspection of CPK and wireframe models of **3** verified that conformer interconversion is sterically facile and that it would involve the sequential rotational motion of the bipyridine subunits within the interior of the macrocycle. This conclusion is also consistent with the ^1H NMR spectrum of **3** in which all the pyridine protons are strongly shielded relative to those of the uncyclised precursors **9**, **10** and **12**.

A variable temperature study of the ^1H NMR spectrum of **3** in $\text{CDCl}_2\text{CDCl}_2$ (Figure 4) revealed that the solution dynamics of this macrocycle is partly different from those of **2** and **9**. Raising the temperature from 0 to 120°C caused the chemical shifts of all the pyridine protons to progressively move

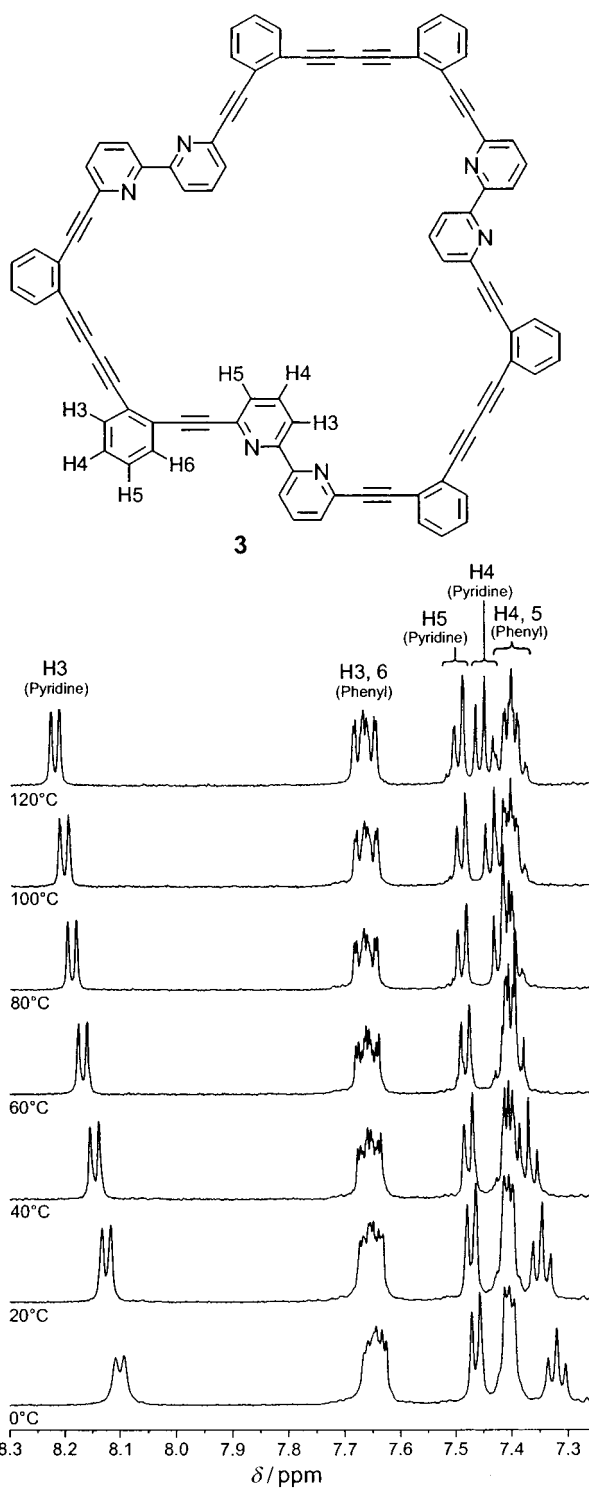


Figure 4. Variation in the chemical shifts of the protons of **3** with temperature. The ¹H NMR spectra were recorded at 500 MHz in CDCl₂CDCl₂.

downfield. The greatest reduction in shielding was experienced by the pyridine H3 and H4 protons, which moved downfield by $\Delta\delta = 0.093$ and 0.103 ppm, respectively, on increasing the temperature from 20–120 °C. The magnitude of these thermally induced downfield shifts are much greater than those of the pyridine H3 and H4 protons of **2** and **9**, and presumably reflects a greater degree of conformational

interconversion and opening of macrocycle **3**. This suggests that the pyridine H3 and H4 protons spend comparatively more time on the NMR timescale pointing towards the interior of the folded framework of **3** at lower temperatures.^[40]

Metal-ion sensing by twistophane 2: To evaluate the metal-ion sensing capabilities of **2**, a detailed spectroscopic investigation into its cation-binding properties was undertaken.

The UV/visible spectrum of uncomplexed **2** in CHCl₃ exhibits five absorbances at 285, 298, 318, 341 and 373 nm, which are invariant in energy and shape over the concentration range of 2.2×10^{-6} – 2.2×10^{-5} mol dm⁻³; this shows that aggregation does not occur in dilute solution. However, all bands do undergo a slight hypsochromic shift when the spectrum of **2** is recorded in 1:2 CHCl₃/MeOH (see Experimental Section).

UV/visible spectra were then recorded of 1:1 stoichiometric mixtures of **2**/Mⁿ⁺ in 1:2 CHCl₃/MeOH, in which $[\mathbf{2}] = 1.09 \times 10^{-5}$ mol dm⁻³ and Mⁿ⁺ = Li^I, Na^I, K^I, Mg^{II}, Ca^{II}, Cr^{III}, Mn^{II}, Fe^{II}, Co^{II}, Ni^{II}, Pd^{II}, Pt^{II}, Zn^{II}, Cd^{II}, Hg^{II}, Pb^{II}, Tl^I, Al^{III}, In^{III}, Sc^{III}, Y^{III}, La^{III}, Eu^{III}, Tb^{III} and NH₄⁺.^[41] All spectra showed zero or negligible changes relative to the UV/visible spectrum of **2**; this indicates insignificant binding of the macrocycle to the above cations in dilute solution. However, the UV/visible spectra of stoichiometric 1:1 combinations of **2**/Cu^{II} and **2**/Ag^I in 1:2 CHCl₃/MeOH, in which $[\mathbf{2}] = 1.09 \times 10^{-5}$ mol dm⁻³, were significantly different from the spectrum of pure **2**, demonstrating that coordination of these ions was occurring. In both cases, the spectral changes involved a drastic reduction in the intensity of all absorption maxima of **2**, and a shift to lower energy of the 317 nm band of the free ligand. The strengths and intensities of the coordination-induced spectral changes of **2** are exemplified by comparison with the spectra of free 2,2'-bipy and 1:1 mixtures of 2,2'-bipy:Cu^{II} and 2,2'-bipy:Ag^I in 1:2 CHCl₃/MeOH, in which $[2,2'\text{-bipy}] = 1.09 \times 10^{-5}$ mol dm⁻³ (Figure 5). The latter comparison demonstrates the importance of the extended, cyclic conjugation of **2** in amplifying the spectroscopic response to metal-ion

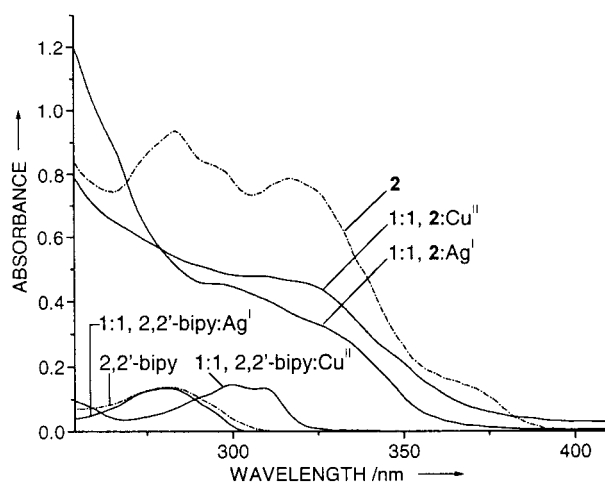


Figure 5. UV/Vis absorption spectra of 1:1, **2**/Mⁿ⁺ in 1:2 CHCl₃/MeOH, in which Mⁿ⁺ = Ag^I and Cu^{II} and $[\mathbf{2}] = 1.09 \times 10^{-5}$ mol dm⁻³. The spectra of 1:1 mixtures of Mⁿ⁺ with 2,2'-bipyridine in 1:2 CHCl₃/MeOH at identical concentrations are also included for comparison.

binding events. A 1:1:1 mixture of **2**/Cu^{II}/Ag^I in 1:2 CHCl₃/MeOH, where [2] = 1.09 × 10⁻⁵ mol dm⁻³, produced a spectrum intermediate in shape between those of the separate 1:1 combinations of **2**/Cu^{II} and **2**/Ag^I. This competitive binding experiment therefore showed that the complexation preference of **2** for Cu^{II} versus Ag^I is approximately equal.

A particularly surprising observation was that the UV/visible spectra of 1:1 mixtures of **2**/Cu^{II} and **2**/Ag^I in 1:2 CHCl₃/MeOH, in which [2] = 1.09 × 10⁻⁵ mol dm⁻³, decayed irreversibly upon standing for several days, finally reaching a limiting situation in which virtually all spectral absorptions had disappeared. This slow, time-dependent spectral decay phenomenon was also displayed by 1:1 mixtures of **2** with apparently non-coordinating metal ions such as Mn^{II}, Fe^{II}, Zn^{II}, Cd^{II}, Hg^{II} and In^{III}. To obtain further insight into the origin of this apparent instability of **2** towards particular metal ions, the **2**/Ag^I system was selected for study in greater detail. Thus when solutions of **2**/Ag^I in 1:2 CHCl₃/MeOH were prepared with incrementally increasing proportions of Ag^I, the maximal spectral changes occurred up to a ratio of 1:1. A slow reduction in the absorbance of all titration curves (to differing degrees) occurred within the first 0.5 h of mixing. This change was, however, reversible, as addition of excess aq. KCN completely regenerated the original spectrum of uncomplexed **2** in every case. These initial spectral changes must therefore be attributable to the slow kinetics of the binding mechanism of Ag^I to **2**. After 0.5 h from mixing, the addition of excess aq. KCN regenerates the spectrum of **2** with reduced absorbances, showing that irreversible changes have begun to take place. The spectral decay process is also catalytic in Ag^I as a 1:0.1 combination of **2**/Ag^I in 1:2 CHCl₃/MeOH underwent a significant reduction in absorbance upon standing for seven days (Figure 6). The fact that a catalytic

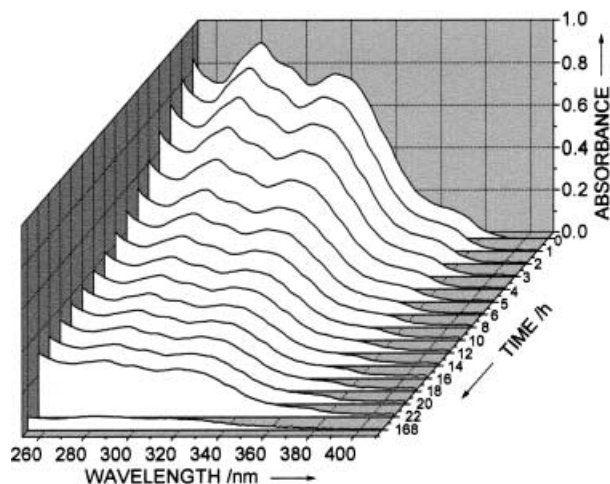


Figure 6. Time dependent decay of the UV/Vis absorption spectrum of a 1:0.1 ratio of **2**/Ag^I with [2] = 1.09 × 10⁻⁵ mol dm⁻³ in 1:2 CHCl₃/MeOH.

amount of Ag^I causes an almost complete extinction in absorbance of **2** demonstrates that the process is not due to the formation and precipitation of a coordination polymer, as this would require at least a stoichiometric quantity of Ag^I ions. The phenomenon is, therefore, most likely to result from a chemical reaction in which **2** itself either decomposes or

polymerises. The Ag^I-ion-induced spectral decay of **2** also occurs in the dark, ruling out possible photochemical origins. The precise reason for the metal-ion-induced destruction of **2** is presently unknown, but suggests intriguingly, that **2** may be able to exist in more strained and energetically enhanced conformations than those predicted by AM1 calculations. The low yield of **2** may also be partly attributable to an instability towards the copper catalyst involved in the oxidative coupling of **10**.

Solutions of **2** in organic solvents emit a blue-purple fluorescence when irradiated with UV light. The fluorescence emission of **2** in deoxygenated CHCl₃ is composed of two maxima at 391 and 419 nm when excited at the wavelength of the absorption envelope at 318 nm. The energies of the emission maxima remained unchanged over the concentration range of 1 × 10⁻⁶–1 × 10⁻⁵ mol dm⁻³; this shows that aggregation of the excited state does not occur in dilute solution. Changing the solvent to aerated 1:2 CHCl₃/MeOH also had a negligible effect upon the emission spectrum of **2**. Fluorescence emission spectra of 1:1 solutions of **2**/Mⁿ⁺ in 1:2 CHCl₃/MeOH were then recorded, where [2] = 1 × 10⁻⁵ mol dm⁻³ and Mⁿ⁺ = all cations and metal chlorides investigated in UV/visible spectroscopic studies described above. Of all metals examined, only Cu^{II} and Ag^I evoked changes in the fluorescence emission of **2**, and in each case caused quenching of the fluorescence of the macrocycle. The fluorescence quenching is illustrated for the **2**/Ag^I system, which shows the spectra of solutions of **2** with increasing incremental additions of Ag^I (Figure 7). From this titration experiment, the detection limit for silver ions was estimated to be at [Ag^I] = 1 × 10⁻⁶ mol dm⁻³.

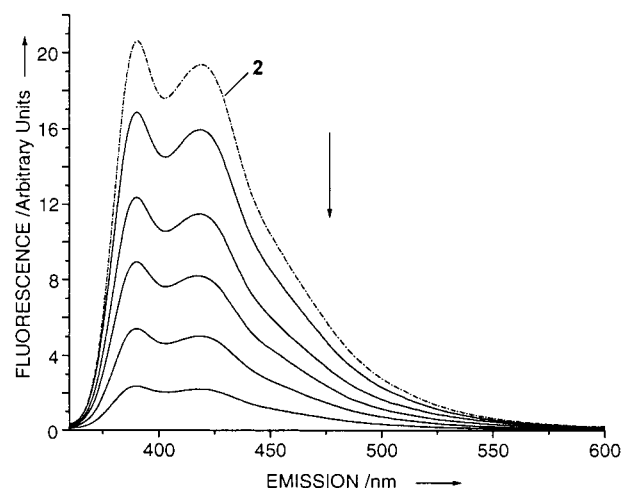


Figure 7. Fluorescence emission spectra of **2** with successive incremental additions of Ag^I with [2] = 1.09 × 10⁻⁵ mol dm⁻³ in 1:2 CHCl₃/MeOH and **2**/Ag^I ratios of 1:0.2, 1:0.4, 1:0.6, 1:0.8 and 1:1.

Twistophane **2** is therefore a particularly selective complexant in dilute solution, binding to only two of the twenty-seven cations and metal chlorides studied. As a result, **2** also functions as a selective sensor for Cu^{II} and Ag^I ions signalling their presence through a fluorescence quenching output response.

Metal-ion sensing by twistophane 3: The metal-ion binding capabilities of **3** would be expected to be significantly different from those of **2**, due to the greater degree of conformational freedom available to the former macrocycle. To determine the effect of increased conformational mobility on the selectivity of the metal-ion sensing response, a spectroscopic investigation into the complexation properties of **3** was undertaken. The UV/visible spectrum of **3** in deoxygenated CHCl_3 is composed of five envelopes at 285, 297, 318, 341 and 365 nm which remained identical in shape and energy over the concentration range of 2.9×10^{-6} – 3.6×10^{-5} mol dm^{-3} , showing that aggregation does not occur in dilute solution. When the spectrum of **3** is recorded in 1:2 $\text{CHCl}_3/\text{MeOH}$ the three highest energy bands undergo a slight hypsochromic shift (see Experimental Section).

The metal-ion binding experiments were conducted by using 1:1.5 ratios of $\mathbf{3}/\text{M}^{n+}$ in 1:2 $\text{CHCl}_3/\text{MeOH}$ in which $[\mathbf{3}] = 7.3 \times 10^{-6}$ mol dm^{-3} and $\text{M}^{n+} =$ all cations and metal chlorides investigated in the spectroscopic studies of **2** above. Of all analytes investigated, only Cu^{II} , Ag^{I} , Hg^{II} , Pd^{II} and Tl^{I} engendered changes in the UV/visible spectrum of **3** (Figure 8). The first four analytes caused a reduction in the

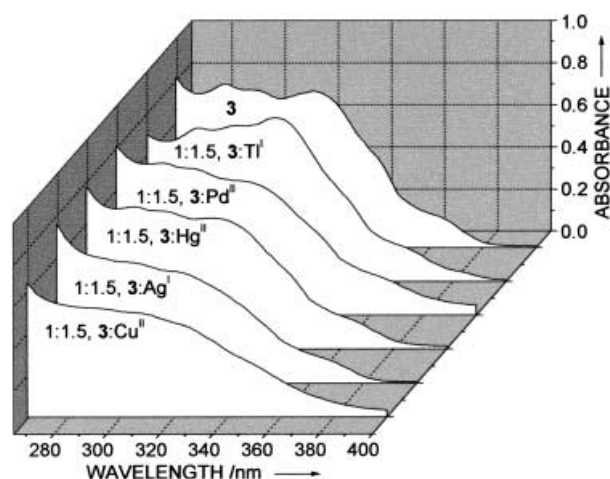


Figure 8. UV/Vis absorption spectra of 1:1.5 ratios of $\mathbf{3}/\text{M}^{n+}$ in 1:2 $\text{CHCl}_3/\text{MeOH}$ in which $[\mathbf{3}] = 7.3 \times 10^{-6}$ mol dm^{-3} , and $\text{M}^{n+} = \text{Cu}^{\text{II}}$, Ag^{I} , Hg^{II} , Tl^{I} and Pd^{II} .

strongest absorption envelopes of **3**, with Cu^{II} and Ag^{I} producing the greatest coordination induced changes. In contrast, Tl^{I} caused a simultaneous increase in absorbance and shift to higher energy of the 316 nm band of **3**. A titration experiment performed on the $\mathbf{3}/\text{Ag}^{\text{I}}$ system, revealed that addition of further aliquots of Ag^{I} caused only minor changes in the UV/visible spectrum once the 1:1.5 $\mathbf{3}/\text{Ag}^{\text{I}}$ ratio was passed. This result suggests that the main reaction product is probably a species of stoichiometry $[\text{Ag}(\mathbf{3})]^+$, in which two of the bipyridine subunits of **3** are coordinated to a single Ag^{I} ion. Modelling studies supported this conclusion and showed that binding of two bipyridine subunits to the same Ag^{I} ion causes the third bipyridine to be locked into a *transoid* conformation and therefore unavailable for further coordination.^[42]

To reveal the ion-binding selectivity of **3**, competitive ion-complexation studies were conducted using 1:1.5:1.5 mixtures of $\mathbf{3}/\text{M}^{n+}/\text{M}^{2n+}$ in 1:2 $\text{CHCl}_3/\text{MeOH}$, in which $[\mathbf{3}] = 7.3 \times 10^{-6}$ mol dm^{-3} . The binding preference of **3** to the five metal species was thus found to follow the qualitative sequence $\text{Cu}^{\text{II}} \approx \text{Ag}^{\text{I}} > \text{Pd}^{\text{II}} > \text{Tl}^{\text{I}} > \text{Hg}^{\text{II}}$, arranged in order of decreasing binding strength. In the case of Pd^{II} , the measurements were hampered by slow binding kinetics. For example, Cu^{II} initially preferentially coordinated to **3** in the presence of Pd^{II} , but after 10 h the degree of binding of the two species to **3** was approximately equal. Slow binding kinetics was also observed in the 1:1.5, $\mathbf{3}/\text{Hg}^{\text{II}}$ system, in which gradual changes in the UV/visible spectrum continued to take place up to 36 h after mixing.

Interestingly, the irreversible metal-ion-induced spectral decay phenomenon exhibited by **2** was not observed to occur with any 1:1.5 $\mathbf{3}/\text{M}^{n+}$ combinations. This finding supports the conclusion that the instability of the former macrocycle towards certain metal ions may originate from a unique structural feature within **2** such as inherent ring strain.

Similarly to **2**, solutions of **3** in organic solvents emit a blue-purple fluorescence when irradiated with UV light. The fluorescence emission of **3** in deoxygenated CHCl_3 is composed of a single maximum at 400 nm when excited at the energy of the absorption envelope at 318 nm. The latter emission maximum remained unchanged in energy at $[\mathbf{3}] \leq 2.9 \times 10^{-6}$ mol dm^{-3} , showing that aggregation of the excited state does not occur in dilute solution. The fluorescence emission spectrum of **3** recorded in aerated 1:2 $\text{CHCl}_3/\text{MeOH}$ at $[\mathbf{3}] \leq 2.9 \times 10^{-6}$ mol dm^{-3} , also consists of a single but much broader emission envelope, which was shifted to slightly lower energy.

Fluorescence emission spectra of 1:1 mixtures of $\mathbf{3}/\text{M}^{n+}$ in 1:2 $\text{CHCl}_3/\text{MeOH}$ were then recorded, in which $[\mathbf{3}] = 2.9 \times 10^{-6}$ mol dm^{-3} and $\text{M}^{n+} = \text{Cu}^{\text{II}}$, Ag^{I} , Hg^{II} and Pd^{II} . The qualitative changes in the fluorescence emission of **3** were as follows: Cu^{II} caused almost complete quenching, Ag^{I} and Pd^{II} caused partial quenching and Hg^{II} produced slight quenching. A titration experiment, in which the spectra of solutions of **3** with incremental additions of Cu^{II} were recorded, enabled an estimation of the sensory detection limit for Cu^{II} to be at $[\text{Cu}^{\text{II}}] = 6 \times 10^{-7}$ mol dm^{-3} (Figure 9). These measurements were again accompanied by time-dependent changes in the fluorescence maxima, which involved slow and continually increased quenching during the first hour after mixing.

The 1:1 $\mathbf{3}/\text{Ag}^{\text{I}}$ system in 1:2 $\text{CHCl}_3/\text{MeOH}$ exhibited particularly curious time-dependent variations in the fluorescence maximum (Figure 10). Initially, a rapid partial quenching of the fluorescence of **3** ensued directly after mixing with silver ions. After 5 min however, the fluorescence began to return, and by 1.5 h had become slightly greater in intensity than that of the emission maximum of **3** prior to mixing. This change was also accompanied by the growth of a lower energy emission envelope at 550 nm. The latter observation of a nonlinear time-dependent change in emissive species suggests that they are being generated by a reaction mechanism between **3** and metal ions that is more complex than originally anticipated. The expanded range of conformational states available to **3**, coupled with the additional ability

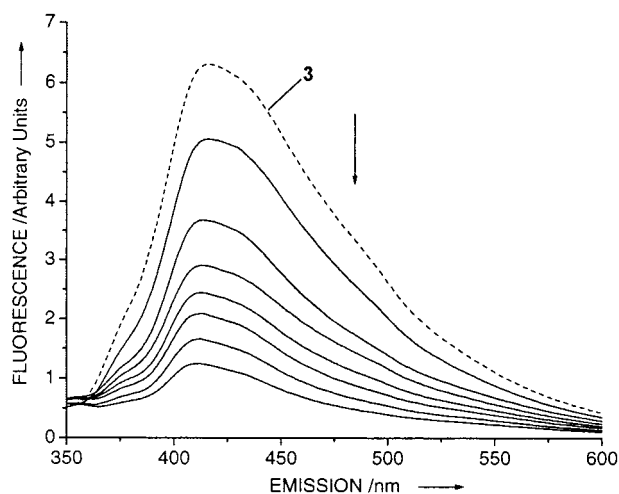


Figure 9. Fluorescence emission spectra of **3** with successive incremental additions of Cu^{II} with $[\mathbf{3}] = 2.9 \times 10^{-6} \text{ mol dm}^{-3}$ in 1:2 $\text{CHCl}_3/\text{MeOH}$ and $\mathbf{3}/\text{Cu}^{\text{II}}$ ratios of 1:0.2, 1:0.4, 1:0.6, 1:0.8, 1:1, 1:2 and 1:3.

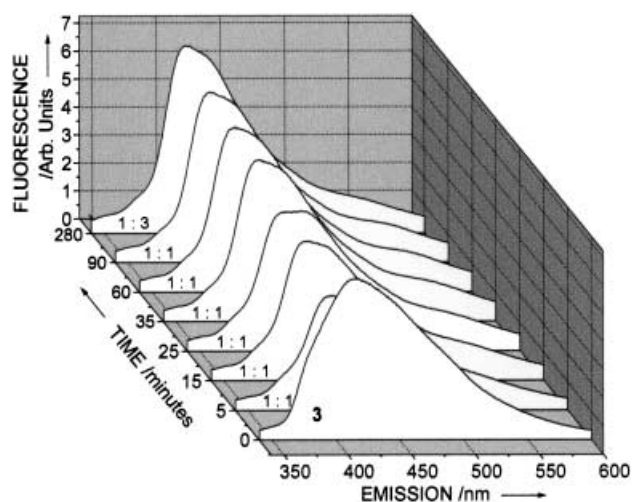


Figure 10. Time-dependent changes in the fluorescence emission spectrum of a 1:1 ratio of $\mathbf{3}/\text{Ag}^{\text{I}}$ with $[\mathbf{3}] = 2.9 \times 10^{-6} \text{ mol dm}^{-3}$ in 1:2 $\text{CHCl}_3/\text{MeOH}$. After 90 min ageing, the $\mathbf{3}/\text{Ag}^{\text{I}}$ ratio was adjusted to 1:3 and the final spectrum recorded at 280 min from the initial mixing of **3** with Ag^{I} . (The $\mathbf{3}/\text{Ag}^{\text{I}}$ ratios are shown on each spectrum).

of Cu^{II} , Ag^{I} , Hg^{II} and Pd^{II} to form interactions of varying strength with alkynes and in some cases phenyl rings,^[18c, 43a-c] indicates that a large number of ground and excited state coordination structures may potentially be accessible to **3**. The mechanism of complexation of a given cation by **3** may therefore involve multiple sequential hopping or riding of ions over the cyclophane framework as it passes through different conformations, until the final thermodynamically preferred species or mixture of entities are formed.

In summary, **3** was found to bind to five out of the twenty-seven cations and metal chlorides studied. In terms of the number of different analytes that a ligand is able to bind, **3** is a less selective complexant than **2** in dilute solution. Twistophane **3** binds most strongly to Cu^{II} and Ag^{I} , but similarly to **2**, cannot discriminate between them. However, of all four coordinating metal species, Cu^{II} produced the most intense and enduring fluorescence quenching response. With respect to the signal output, **3** thus gives a single type of output

response characteristic to Cu^{II} . Macrocycle **3** may therefore be considered to be a more selective sensor than **2**, as the latter ligand gives identical signal outputs for two different analytes (i.e., Cu^{II} and Ag^{I}).

Proton sensing by twistophane 3: Protonation of **2**, **3** and **9** also caused changes in the energy and intensity in their respective fluorescence emission spectra. Macrocycle **3** was particularly sensitive in this respect, emitting a turquoise or green fluorescence upon irradiation with UV light when dissolved in aged batches of CHCl_3 . This effect was discovered to originate from the presence of HCl , which is a product from the slow photochemical decomposition of CHCl_3 . In a qualitative investigation of this process, excess CF_3COOH was added to a $2.9 \times 10^{-6} \text{ mol dm}^{-3}$ solution of **3** in 1:2 $\text{CHCl}_3/\text{MeOH}$ and the fluorescence emission spectrum monitored with time (Figure 11). As in the case of silver ion coordination

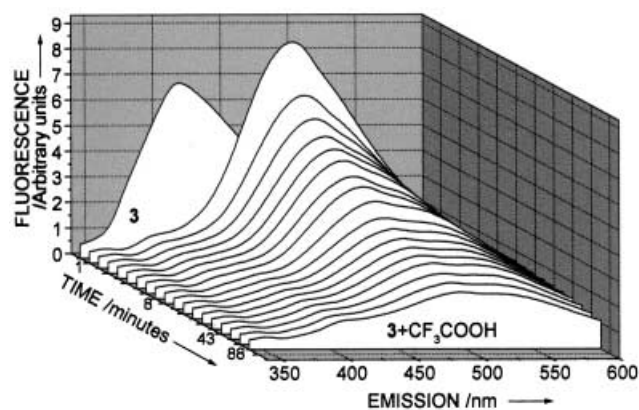


Figure 11. Time-dependent changes in the fluorescence emission spectrum of a solution of **3** ($2.9 \times 10^{-6} \text{ mol dm}^{-3}$) in 1:2 $\text{CHCl}_3/\text{MeOH}$; 0.1 mol dm^{-3} in CF_3COOH . (The spectra were recorded at 1 min intervals between 0 and 8 min; at 5 min intervals between 8 and 43 min; and at 15 min intervals between 43 and 88 min ageing).

to **3**, the emission maximum of the protonated macrocycle changed considerably with time. Thus upon addition of CF_3COOH to **3**, the absorption maximum underwent a sudden simultaneous increase in intensity and shift to lower energy over the first few seconds after mixing. The new fluorescence maximum then gradually decayed with time, eventually becoming much less intense than the original fluorescence envelope of **3**. This was also accompanied by the development of an additional fluorescence envelope at lower energy. Addition of excess aq. K_2CO_3 resulted in complete regeneration of the original emission maximum of **3**, unambiguously demonstrating that the fluorescence changes originated from protonation equilibria and not irreversible chemical reactions.

These time-dependent spectral changes suggest that the protonation of **3** involves the generation of several emissive species, the most kinetically stable of which are formed initially, and which then redistribute over time to the thermodynamically favoured speciation profile.

Metal-ion sensing by precursor 9: Finally, a comparative spectroscopic investigation into the metal-ion binding properties of acyclic precursor **9** was undertaken in order to assess the effect of macrocyclisation on the complexation and sensory capabilities of **2** and **3**. The UV/visible spectra of **9** in CHCl_3 and 1:2 $\text{CHCl}_3/\text{MeOH}$ consists of three bands, and are, therefore, simpler than those of **2** and **3** recorded in the same solvents. The metal-ion binding experiments were conducted by using a 1:0.5 ratio of $9/M^{n+}$ in 1:2, $\text{CHCl}_3/\text{MeOH}$ in which $[9] = 2.2 \times 10^{-5} \text{ mol dm}^{-3}$ and $M^{n+} =$ all cations and metal chlorides investigated in the spectroscopic studies of **2** and **3** above. Similarly to **3**, only Cu^{II} , Ag^{I} , Hg^{II} , and Pd^{II} produced changes in the UV/visible spectrum of **9**. The presence of Cu^{II} , Ag^{I} and Pd^{II} caused reductions in the absorbances of **9** (Figure 12). However, the $9/\text{Hg}^{\text{II}}$ system

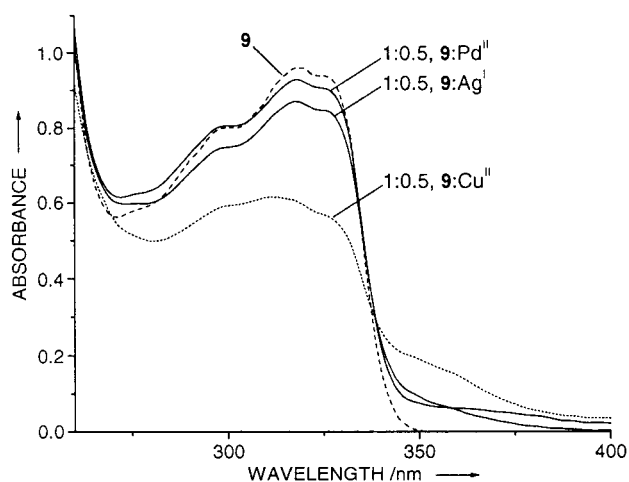


Figure 12. UV/Vis absorption spectra of 1:0.5 ratios of $9/M^{n+}$ in 1:2 $\text{CHCl}_3/\text{MeOH}$, in which $M^{n+} = \text{Ag}^{\text{I}}$, Cu^{II} and Pd^{II} , with $[9] = 2.2 \times 10^{-5} \text{ mol dm}^{-3}$.

exhibited slow time-dependent changes in which the absorptions of **9** at 319 and 326 nm decreased over the first 0.5 h, and by 24 h a new absorption had appeared at 306 nm (Figure 13).

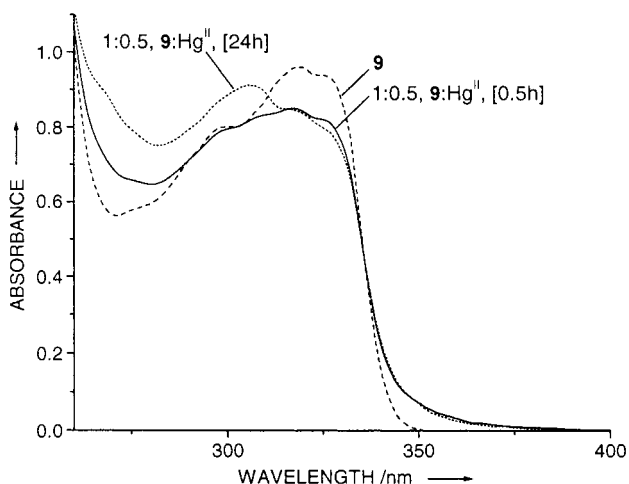


Figure 13. Time-dependent changes in the UV/Vis absorption spectrum of the 1:0.5, $9/\text{Hg}^{\text{II}}$ system with $[9] = 2.2 \times 10^{-5} \text{ mol dm}^{-3}$ in 1:2 $\text{CHCl}_3/\text{MeOH}$.

Having established the metal-ion coordination preferences of **9**, the complexation selectivity was then investigated using 1:0.5:0.5 mixtures of $9/M1^{n+}/M2^{n+}$ in 1:2 $\text{CHCl}_3/\text{MeOH}$, in which $[9] = 2.2 \times 10^{-5} \text{ mol dm}^{-3}$. These competition studies showed that the binding selectivity followed the qualitative sequence $\text{Cu}^{\text{II}} > \text{Pd}^{\text{II}} > \text{Ag}^{\text{I}} \approx \text{Hg}^{\text{II}}$, arranged in order of decreasing binding strength. This series was constructed from measurements taken within the first three minutes of mixing, as the selectivities of some of the reactions again continued to change further over time. For example, the spectrum of the $9/\text{Cu}^{\text{II}}/\text{Pd}^{\text{II}}$ system evolved over 0.5 h into a new spectrum that was completely different to both the 1:0.5, $9/\text{Cu}^{\text{II}}$ and $9/\text{Pd}^{\text{II}}$ spectra (Figure 14). In addition, the reaction solution became

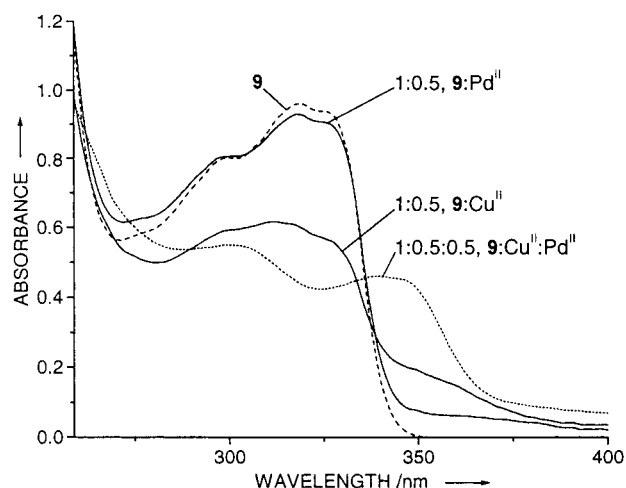


Figure 14. UV/Vis absorption spectra of 1:0.5 ratios of $9/\text{Cu}^{\text{II}}$ and $9/\text{Pd}^{\text{II}}$, and a 1:0.5:0.5 ratio of $9/\text{Cu}^{\text{II}}/\text{Pd}^{\text{II}}$ in 1:2 $\text{CHCl}_3/\text{MeOH}$ with $[9] = 2.2 \times 10^{-5} \text{ mol dm}^{-3}$.

yellow. This finding suggests that the product or products of the reaction between **9**, Cu^{II} and Pd^{II} are chemically very different from those generated from **9** and the metal species separately. The $9/\text{Cu}^{\text{II}}/\text{Pd}^{\text{II}}$ system may therefore be forming products of a higher structural complexity such as aggregates or clusters, composed of multiple ligands simultaneously coordinated to Cu^{II} and Pd^{II} .

The fluorescence response of **9** to metal ions was also investigated under identical conditions to those of the UV/visible spectroscopic metal-ion binding studies of **9** above. These investigations showed that the coordinating analytes Ag^{I} , Hg^{II} and Pd^{II} had a zero or negligible effect upon the fluorescence emission of **9**, whereas Cu^{II} caused partial fluorescence quenching.

Thus ligand **9** binds to four out of the twenty-seven cations and metal chlorides studied and is, therefore, a slightly more selective complexant than **3**, but much less selective than **2**. The binding discrimination of **9** is superior to that of **2** and **3** as it coordinates most strongly to a single metal species (i.e., Cu^{II}). Unlike **3**, precursor **9** on the other hand cannot discriminate between Ag^{I} and Hg^{II} and shows no fluorescence sensory response for these ions. Ligand **9** affords a single, fluorescence output response characteristic of Cu^{II} , and in this respect displays a similar sensory selectivity to **3**, but greater sensory selectivity than **2**. However, the coordination-induced

change in emission intensity, or in other words, the output signal amplification, was qualitatively lower for **9** compared to **2** and **3**, reflecting the greater degree of conjugation in the macrocyclic structures.

Conclusion

The above work discloses the successful preparation of macrocyclic dimer **2** and trimer **3**, which are the first reported examples of 6,6'-connected-2,2'-bipyridyl twistophanes. These molecules represent a new type of cyclically conjugated metal-ion binding scaffold capable of existing in a range of conformational states depending upon the mode and degree of metal-ion coordination. The characterisation of **2** and **3** as macrocyclic entities was based upon MS, and IR and NMR spectroscopic evidence. Variable temperature NMR experiments suggested that **3** was a conformationally mobile entity, exhibiting shielding effects for particular protons, characteristic of motions in and out of the macrocyclic rings. Molecular modelling studies identified the lowest energy conformational states of **2** and **3** as helically twisted and chiral architectures.

It was anticipated that **2** and **3** would function as particularly efficient metal-ion sensors due to their enhanced cyclic conjugation, electronically linked coordination sites and potential for undergoing complexation-induced mechano-structural changes. Subsequent spectroscopic investigations confirmed that **2** and **3** do indeed function as metal-ion sensors. Cyclophane **2** acts as a fluorescence-quenching sensor for Cu^{II} and Ag^I, and **3** as a fluorescence-quenching sensor for Cu^{II}. The acyclic precursor **9** was also found to respond to Cu^{II} by fluorescence quenching but to a qualitatively lesser degree.^[44a-c] The metal-ion binding and sensory properties of **2**, **3** and **9** were found to be subtly different, being best compared and summarised using four descriptors as follows: complexation selectivity, **2** ≫ **9** > **3**; complexation discrimination, **9** > **2** ≈ **3**; sensory selectivity, **3** ≈ **9** > **2** and output signal intensity, **2** ≈ **3** > **9**.^[45] The overall ability of structures such as **2**, **3** and **9** to function as sensors depends, therefore, on a complex interplay of steric, structural and electronic factors such as, for example, the degree of conjugation, the type of conjugation pathway, the electronic nature and position of substituents, intramolecular strain, the number of accessible conformations, the number and accessibility of binding sites and binding site preorganisation.^[46]

Many of the reactions studied exhibited prolonged time-dependent spectral changes upon complexation, indicative of slow binding kinetics. This, however, did not adversely affect the sensory capabilities of **2**, **3** and **9** as coordination-induced fluorescence responses invariably occurred immediately upon contact with the analyte.

Interestingly, **2**, **3** and **9** also function as chromogenic fluorescence sensors for protons, a finding that suggests that these and structurally related compounds may have applications in the field of molecular protonics.

The unique structural features of the conjugated ligands described above, endow these molecules with the ability to signal the presence of particular metal ions through characteristic fluorescence output responses. They therefore constitute

a new lead class of ion sensors that may find a rich variety of applications in the fields of supramolecular sensorics and ionics, as well as related areas such as catalysis, materials science and nanotechnology.^[47]

Experimental Section

General: Standard inert atmosphere and Schlenk techniques were employed for reactions conducted under argon. The catalysts [Pd(PPh₃)₄],^[48] [PdCl₂(PPh₃)₂],^[49] [PdCl₂(dppf)]·CH₂Cl₂,^[50] CuI, CuCl and [Cu₂(OAc)₄] were purchased from Aldrich and used as received. Precursors **4**,^[51] **8**^[27a] and **11**^[55] were prepared according to published procedures. The toluene, THF and triethylamine used in the preparation of **6**, **9** and **12** were deoxygenated by bubbling with argon for 0.5 h directly prior to use. The alumina used for the chromatographic purification of macrocycles **2** and **3** was purchased from Merck (Aluminium Oxide 90, standardised activity II/III). The silica used for all flash chromatography was also purchased from Merck (Geduran, Silica gel Si 60, 40–60 μm).

Intramolecular proton connectivities were determined by ¹H–¹H COSY and NOESY NMR measurements, and carbon assignments of **2** and **12** by ¹H–¹³C HMQC experiments. All ¹H and ¹³C NMR spectra were referenced to the solvent peaks (in the former case, to those of the residual nondeuterated solvent). The fluorescence emission spectra were recorded at 20–25 °C on a Aminco, Bowman Series 2 luminescence spectrophotometer (SLM Instruments, Inc.). The free ligand fluorescence emission spectra of **2**, **3**, **9**, **10** and **12** given below were recorded in argon-bubbled CHCl₃ and were corrected for the instrumental response. The fluorescence emission spectra of the metal-ion binding experiments with **2**, **3** and **9** were conducted in aerated 1:2 CHCl₃/MeOH, in order to obtain optical responses under environmental conditions of most practical utility for sensory applications. The metal-ion binding emission spectra for **2** and **9** recorded under these conditions were corrected for the instrumental response. All infrared spectra were recorded as KBr discs. Melting point measurements were performed on an Electrothermal Digital melting point apparatus calibrated with standards of known melting points. Elemental analyses were performed by the Service de Microanalyse, Institut de Chimie, Université Louis Pasteur (France).

6,6'-Bis(trimethylsilylethynyl)-2,2'-bipyridine (6): Toluene (15 mL), which had been bubbled with argon, was added by syringe to a mixture of **4** (0.434 g, 1.38 × 10⁻³ mol), **5** (1.8 g, 4.65 × 10⁻³ mol) and [Pd(PPh₃)₄] (0.030 g, 2.6 × 10⁻⁵ mol) under an argon atmosphere. The reaction was placed in an oil bath, and refluxed and stirred at 122 °C for 36 h. During heating the reaction turned black. All solvent was then removed under reduced pressure on a water bath, and the residue was purified by flash chromatography on a column of silica, eluting with CH₂Cl₂. The product eluted as a single component, free from accompanying contaminants. The CH₂Cl₂ was removed by distillation at atmospheric pressure on a water bath and the remaining product dried under vacuum (0.01 mm Hg) overnight to yield **6** (0.302 g, 63 %) as a cream crystalline solid. ¹H NMR (CDCl₃, 500 MHz, 25 °C): δ = 8.428 (dd, ³J(3,4) = 8.0 Hz, ⁴J(3,5) = 0.9 Hz, 2H; pyridine H3), 7.758 (t, ³J(4,3;4,5) = 7.8 Hz, 2H; pyridine H4), 7.485 (dd, ³J(5,4) = 7.7 Hz, ⁴J(5,3) = 0.9 Hz, 2H; pyridine H5), 0.294 ppm (s, 18H; Si(CH₃)₃); EIMS: *m/z* (%): 348 (96) [M⁺], 333 (100) [M⁺ – CH₃].

6,6'-Bis(2-trimethylsilylethynylphenyl)ethynyl)-2,2'-bipyridine (9): Toluene (100 mL), which had been bubbled with argon, was added by syringe to a mixture of **7** (0.789 g, 3.86 × 10⁻³ mol), **8** (2.42 g, 8.06 × 10⁻³ mol) and [PdCl₂(dppf)]·CH₂Cl₂ (0.078 g, 9.55 × 10⁻⁵ mol) under an argon atmosphere. The suspension was then placed in a bath at 75 °C and stirred for 0.25 h, that is, until **7** had completely dissolved. A solution of CuI (0.045 g, 2.36 × 10⁻⁴ mol) in Et₃N (13 mL) was added by syringe; this initiated the slow formation of a chocolate-brown suspended solid. Directly after addition of the CuI solution, the stirred mixture was allowed to cool to ambient temperature and stirring continued in the dark for 8 d. All solvent was then removed under reduced pressure on a water bath and the residue slurried in 25/75 CH₂Cl₂/hexane and purified by flash chromatography on a column of silica, eluting with 25/75 CH₂Cl₂/hexane. Unreacted **8** eluted initially, and was followed eventually by **9**. The product was thus obtained as a colourless glass after removal of the solvent by distillation on a water

bath and drying under vacuum. Final purification was achieved upon recrystallisation from hexane and drying under vacuum (0.01 mmHg for 24 h), to yield **9** (1.824 g, 86%) as colourless crystals. M.p. 142.4–143.0 °C; ^1H NMR (CDCl_3 , 500 MHz, 25 °C): δ = 8.503 (dd, $^3J(3,4)$ = 7.9 Hz, $^4J(3,5)$ = 0.9 Hz, 2H; pyridine H3), 7.819 (t, $^3J(4,3;4,5)$ = 7.9 Hz, 2H; pyridine H4), 7.636 (m, 2H; phenyl H6), 7.600 (dd, $^3J(5,4)$ = 7.6 Hz, $^4J(5,3)$ = 0.9 Hz, 2H; pyridine H5), 7.531 (m, 2H; phenyl H3), 7.324 (m, 4H; phenyl H4, H5), 0.272 ppm (s, 18H; Si(CH_3)₃); ^{13}C NMR (CDCl_3 , 125.8 MHz, 25 °C): δ = 155.9, 142.8, 136.9, 132.3, 132.2, 128.6, 128.2, 127.8, 126.2, 125.2, 120.9, 103.2 (–C≡), 99.1 (–C≡), 92.6 (–C≡), 87.7 (–C≡), 0.0 ppm (Si(CH_3)₃); UV/Vis (CHCl_3): λ_{max} (ϵ) = 301 (42145), 319 (48580), 328 nm (47606 $\text{m}^{-1}\text{cm}^{-1}$); fluorescence emission ([**9**] = 1.46×10^{-6} mol dm^{-3} in CHCl_3 , 319 nm excitation): λ_{max} = 342 nm; IR: $\tilde{\nu}$ = 2954 (s), 2218 (w) (C=C), 2160 (s) (C=C), 1568 (s), 1560 (s), 1480 (s), 1431 (s), 1249 (s), 846 (s), 802 (s), 757 cm^{-1} (s); EIMS: m/z (%): 548 (57) [M^+], 533 (20) [M^+ – CH_3], 475 (100) [M^+ – SiMe₃]; elemental analysis calcd (%) for $\text{C}_{30}\text{H}_{32}\text{N}_2\text{Si}_2$: C 78.78, H 5.88, N 5.10; found: C 78.62, H 5.69, N 5.11.

6,6'-Bis[2-[4-(2-methyl-2-hydroxy-3-butynyl)]phenyl]ethynyl-2,2'-bipyridine (12): THF (20 mL), which had been bubbled with argon, was added by syringe to a mixture of **11** (0.286 g, 1.55×10^{-3} mol), **4** (0.235 g, 7.48×10^{-4} mol) and $[\text{PdCl}_2(\text{PPh}_3)_2]$ (0.020 g, 2.85×10^{-5} mol) under an atmosphere of argon. The mixture was stirred for 0.25 h, that is, until **4** had dissolved, and then a solution of CuI (0.014 g, 7.35×10^{-5} mol) in Et_3N (2 mL, bubbled with argon) was added by syringe. Directly after addition of the CuI in Et_3N , the suspended $[\text{PdCl}_2(\text{PPh}_3)_2]$ dissolved to give a yellow solution from which a another suspended solid slowly began to form. The reaction was stirred at ambient temperature for 7 d in the absence of light. All solvent was subsequently removed under reduced pressure on a water bath to give a brown glassy residue, which was purified by flash chromatography on a short column of silica. The column was eluted first with CH_2Cl_2 to remove a contaminant that was visualised as a purple-blue fluorescent band with a fluorescent lamp operating at 365 nm. Gradient elution with 1% MeOH/ CH_2Cl_2 and finally 2% MeOH/ CH_2Cl_2 resulted in removal of **12** from the column. The product **12** was also observable on the column as a strong purple-blue fluorescent band with a fluorescent lamp operating at 365 nm. The product was thus obtained as a clear pale-brown glass after removal of solvent and drying under vacuum. The glass was then dissolved in boiling *n*-heptane (600 mL), NORIT A decolourising charcoal (0.06 g) added, and boiling continued for a further 0.1 h. The mixture was subsequently gravity filtered and left to stand for 24 h. The crystalline solid that separated was isolated by filtration under vacuum, washed with *n*-heptane (4 mL) and air-dried to give **12** (0.200 g, 51%) as a microcrystalline cream solid. M.p. 175.1–175.7 °C; ^1H NMR (CDCl_3 , 500 MHz, 25 °C): δ = 8.417 (dd, $^3J(3,4)$ = 7.5 Hz, $^4J(3,5)$ = 0.8 Hz, 2H; pyridine H3), 7.817 (t, $^3J(4,3;4,5)$ = 7.9 Hz, 2H; pyridine H4), 7.612 (m, 4H; pyridine H5/phenyl H6), 7.448 (m, 2H; phenyl H3), 7.314 (m, 4H; phenyl H4/5), 1.649 ppm (s, 12H; C(CH_3)₂OH); ^{13}C NMR (CDCl_3 , 125.8 MHz, 25 °C): δ = 156.1, 142.8, 137.1 (C4 pyridine), 131.9 (C5 pyridine/C6 phenyl), 131.2 (C3 phenyl), 128.7 (C4/5 phenyl), 127.9 (C4/5 phenyl), 127.7 (C5 pyridine/C6 phenyl), 126.1, 125.3, 121.3 (C3 pyridine), 99.3 (–C≡), 92.6 (–C≡), 87.9 (–C≡), 80.8 (–C≡), 65.6 (C(CH_3)₂OH), 31.4 ppm (C(CH_3)₂OH); UV/Vis (CHCl_3): λ_{max} (ϵ) = 297 (48204), 319 (53143), 326 nm (53833 $\text{m}^{-1}\text{cm}^{-1}$); fluorescence emission ([**12**] = 1.54×10^{-6} mol dm^{-3} in CHCl_3 , 319 nm excitation): λ_{max} = 345 nm; IR: $\tilde{\nu}$ = 3356 (s) (O–H), 2979 (m), 2219 (m) (C=C), 1569 (s), 1560 (s), 1445 (s), 1432 (s), 1169 (s), 1155 (s), 964 (s), 798 (s), 759 cm^{-1} (s); FABMS: m/z (%): 521 (100) [M^+ + H], 505 (20) [M^+ – CH_3]; elemental analysis calcd (%) for $\text{C}_{36}\text{H}_{28}\text{N}_2\text{O}_2$: C 83.05, H 5.42, N 5.38; found: C 83.01, H 5.46, N 5.23.

6,6'-Bis[2-(2-ethynylphenyl)ethynyl]-2,2'-bipyridine (10), (from 9): TBAF (7 mL, 1.0 M solution in THF) was added to a stirred solution of **9** (1.824 g, 3.32×10^{-3} mol) in THF (40 mL) and distilled water (0.5 mL). The clear reaction was then stirred at ambient temperature in the absence of light for 18 h. TLC (CH_2Cl_2 /Silica) of the reaction at this point showed all the **9** to be consumed. All solvent was removed under reduced pressure on a water bath and the residue dissolved in CH_2Cl_2 (50 mL) and extracted with distilled water (4 × 60 mL). The organic layer was separated, dried (anhydrous MgSO_4) and filtered, and the solvent volume reduced to 20 mL by distillation at atmospheric pressure on a water bath. The concentrate was then purified by flash chromatography on a column of silica with CH_2Cl_2 as eluant. The product thus obtained was finally purified by brief ultrasonication in MeOH (4 mL), filtering under vacuum, and washing the collected solid with MeOH (2 mL) followed by air drying to

give **10** (1.309 g, 97%) as a white powder. M.p. 142.5–143.5 °C; ^1H NMR (CDCl_3 , 500 MHz, 25 °C): δ = 8.498 (dd, $^3J(3,4)$ = 8.0 Hz, $^4J(3,5)$ = 0.7 Hz, 2H; pyridine H3), 7.830 (t, $^3J(4,3;4,5)$ = 7.8 Hz, 2H; pyridine H4), 7.661 (m, 2H; phenyl H6), 7.618 (dd, $^3J(5,4)$ = 7.6 Hz, $^4J(5,3)$ = 0.8 Hz, 2H; pyridine H5), 7.569 (m, 2H; phenyl H3), 7.358 (m, 4H; phenyl H4/5), 3.420 ppm (s, 2H; H–C≡C); ^{13}C NMR (CDCl_3 , 125.8 MHz, 25 °C): δ = 155.9, 142.7, 137.0, 132.6, 132.3, 128.64, 128.58, 128.0, 125.4, 125.1, 120.9, 92.7 (–C≡), 87.3 (–C≡), 82.0 (–C≡), 81.5 ppm (–C≡); UV/Vis (CHCl_3): λ_{max} (ϵ) = 297 (39575), 320 nm (44596 $\text{m}^{-1}\text{cm}^{-1}$); fluorescence emission ([**10**] = 1.98×10^{-6} mol dm^{-3} in CHCl_3 , 320 nm excitation): λ_{max} = 340 nm; IR: $\tilde{\nu}$ = 3291 (s) (H–C≡), 2221 (w) (C=C), 1568 (s), 1561 (s) 1478 (s), 1446 (s), 1435 (s), 795 (s), 754 (s), 616 (s); FABMS: m/z (%): 405 (100) [M^+ + H].

6,6'-Bis[2-(2-ethynylphenyl)ethynyl]-2,2'-bipyridine (10), (from 12): Toluene (7 mL), which had been bubbled with argon, was added by syringe to a mixture of **12** (0.043 g, 8.26×10^{-5} mol) and powdered KOH (0.011 g, 1.96×10^{-4} mol) under an atmosphere of argon; the suspended solids were dispersed by brief ultrasonication. The reaction was then stirred and heated in a bath at 110 °C for 7 h, during which time the reaction solution turned pale yellow and some brown solid formed on the flask walls. TLC (1% MeOH/ CH_2Cl_2 , silica) performed at this point showed that **12** had been consumed. The reaction was then poured onto CH_2Cl_2 (25 mL) and extracted with distilled water (2 × 20 mL). The organic layer was dried (anhydrous MgSO_4), filtered and the solvent removed by distillation under reduced pressure on a waterbath. The residue was then dissolved in CH_2Cl_2 (10 mL) and the concentrate was purified by flash chromatography on a column of silica with CH_2Cl_2 as eluant. The product thus obtained was finally purified by dissolving in hot hexane (100 mL), adding NORIT A decolourising charcoal (0.03 g) and briefly boiling followed by gravity filtration. The filtrate was reduced in volume to about 3 mL by distillation under reduced pressure on a waterbath and left to cool to ambient temperature. The mixture was then filtered under vacuum, and the collected solid washed with ice-cold hexane (2 mL) and air-dried to give **10** (0.026 g, 79%) as a white microcrystalline solid. M.p. 145.6–146.6 °C; the ^1H and ^{13}C NMR spectra of the product were identical to those of **10** prepared from **9** as described above; elemental analysis calcd (%) for $\text{C}_{30}\text{H}_{16}\text{N}_2$: C 89.09, H 3.99, N 6.93; found: C 89.08, H 3.94, N 6.83.

Macrocycle 2 (Hay procedure): In a well-ventilated hood, a solution of CuCl (0.023 g, 2.32×10^{-4} mol) in pyridine (2 mL) was added to a solution of **10** (0.167 g, 4.13×10^{-4} mol) in pyridine (230 mL) contained in a ribbed 500 mL three-necked round-bottomed flask, and the reaction solution vigorously stirred and bubbled with oxygen for 14 d. During this time, the volume of the reaction solution evaporated down to about 90 mL. The reaction was subsequently re-diluted to 230 mL by the addition of pyridine and further CuCl (0.025 g, 2.53×10^{-4} mol) added. Oxygen bubbling and vigorous stirring was then continued for a further 11 d, periodically re-diluting to 230 mL with pyridine, whenever evaporation down to 100 mL occurred. During the periods of maximum solvent volume reduction, a suspended solid formed on the flask walls. All solvent was then removed under reduced pressure; a concentrated aqueous KCN solution (20 mL) was then added to the residue and the mixture rapidly stirred for 1 h. The mixture was filtered under vacuum and, the isolated dark brown solid washed with excess distilled water and air-dried. The solid was then suspended in CHCl_3 (250 mL), boiled for 0.1 h, and gravity filtered to remove polymeric by-products; then the solvent was removed by distillation on a water bath at atmospheric pressure. The remaining solid was finally boiled in toluene (150 mL) and the hot mixture introduced onto a 29 × 6.5 cm diameter column of alumina and the column eluted with toluene. The product thus obtained was subject once again to chromatography under identical conditions and suspended in MeOH (3 mL), briefly ultrasonicated, isolated by filtration under vacuum, washed with MeOH and air-dried to give **2** (0.021 g, 13%) as an amorphous off-white powder. ^1H NMR ($\text{CDCl}_2\text{CDCl}_2$, 500 MHz, 20 °C): δ = 8.083 (dd, $^3J(3,4)$ = 7.9 Hz, $^4J(3,5)$ = 0.8 Hz, 4H; pyridine H3), 7.735 (t, $^3J(4,3;4,5)$ = 7.7 Hz, 4H; pyridine H4), 7.658 (m, 8H; phenyl H3/6), 7.609 (dd, $^3J(5,4)$ = 7.6 Hz, $^4J(5,3)$ = 0.8 Hz, 4H; pyridine H5), 7.444 ppm (m, 8H; phenyl H4/5); ^{13}C NMR ($\text{CDCl}_2\text{CDCl}_2$, 125.8 MHz, 80 °C): δ = 154.9, 142.2, 136.9 (C4 pyridine), 132.2 (C3/6 phenyl), 131.8 (C3/6 phenyl), 129.2 (C4/5 phenyl), 128.9 (C5 pyridine), 128.7 (C4/5 phenyl), 127.2, 125.5, 120.6 (C3 pyridine), 94.7 (–C≡), 87.3 (–C≡), 81.9 (–C≡), 78.6 ppm (–C≡); UV/Vis (CHCl_3): λ_{max} (ϵ) = 285 (80637), 298 (sh) (67987), 318 (66496), 341 (sh) (36952), 373 nm (11040 $\text{m}^{-1}\text{cm}^{-1}$); UV/Vis (1:2 CHCl_3 /MeOH): λ_{max} (ϵ) = 284 (85636), 296

(74995), 317 (72068), 340 (42104), 370 nm ($12342\text{ M}^{-1}\text{ cm}^{-1}$); fluorescence emission ($[2] = 9.94 \times 10^{-7}\text{ mol dm}^{-3}$ in CHCl_3 , 318 nm excitation): $\lambda_{\text{max}} = 391, 419\text{ nm}$; IR: $\tilde{\nu} = 2920, 2215\text{ (w)} (\text{C}=\text{C}), 1569\text{ (s)}, 1560\text{ (s)}, 1472\text{ (s)}, 1453\text{ (s)}, 1430\text{ (s)}, 1259\text{ (m)}, 1082\text{ (m)}, 796\text{ (s)}, 753\text{ (s)}, 735\text{ (s)}, 637\text{ cm}^{-1}\text{ (m)}$; FABMS (recorded in 10–20% $\text{CF}_3\text{COOH}/\text{CHCl}_3$): m/z (%): 805 (100) [$M^+ + \text{H}$]; HRMS (FAB, CF_3COOH , [$M^+ + \text{H}$]) calcd for $\text{C}_{60}\text{H}_{29}\text{N}_4$: 805.2392; found: 805.2394.

Macrocycles 2 and 3 (Breslow procedure): A solution of **10** (0.202 g, $4.99 \times 10^{-4}\text{ mol}$) in pyridine (35 mL) was added dropwise over 4 h to a rapidly stirred suspension of CuCl (1.48 g, $1.5 \times 10^{-2}\text{ mol}$) and $[\text{Cu}_2(\text{OAc})_4]$ (3.63 g, $2.0 \times 10^{-2}\text{ mol}$) in pyridine (300 mL), heated in a bath at 60°C . After the addition of **10** was complete, the green mixture was stirred at 60°C for a further 2 h, then allowed to cool to ambient temperature and stirring continued for 14 d. All solvent was then removed under reduced pressure on a waterbath at 70°C and pyridine (15 mL) added to wet the remaining solid residue. A concentrated aqueous solution of KCN (100 mL) was added to the reaction product, and the mixture rapidly stirred for 1 h and filtered under vacuum; then the isolated solid washed with excess distilled water and air-dried. The dark brown solid was then boiled in toluene (900 mL) and gravity filtered while still hot; the filtrate reduced in volume to 200 mL by distillation under reduced pressure on a water bath. The hot solution was introduced onto a large column of alumina and eluted with toluene. The progress of the chromatography was monitored with a fluorescent lamp operating at 365 nm, whereby **2** appeared as the first blue-purple fluorescent band to elute from the column and **3** the second. Each macrocyclic component was then separately subjected once again to chromatography on alumina columns with toluene as eluant. Both macrocycles thus isolated were further purified by boiling each in acetone (10 mL), filtering under vacuum, washing the collected products with acetone and finally air dried to give **2** (0.019 g, 9%) and **3** (0.011 g, 5%) as off-white dusty solids. Characterisation data for **3**: $^1\text{H NMR}$ ($\text{CDCl}_2\text{CDCl}_2$, 500 MHz, 20°C): $\delta = 8.126\text{ (d, }^3J(3,4) = 8.0\text{ Hz, 6H; pyridine H3}), 7.652\text{ (m, 12H; phenyl H3/6)}, 7.472\text{ (d, }^3J(5,4) = 7.8\text{ Hz, 6H; pyridine H5)}, 7.406\text{ (m, 12H; phenyl H4/5)}, 7.346\text{ ppm (t, }^3J(4,3;4,5) = 7.8\text{ Hz, 6H; pyridine H4)}$; $^{13}\text{C NMR}$ ($\text{CDCl}_2\text{CDCl}_2$, 125.8 MHz, 120°C): $\delta = 155.8, 142.3, 136.6, 132.8, 132.2, 128.9, 128.4, 127.7, 126.8, 125.4, 120.8, 94.6$ ($-\text{C}=\text{C}$), 86.9 ($-\text{C}=\text{C}$), 81.7 ($-\text{C}=\text{C}$), 78.7 ppm ($-\text{C}=\text{C}$); UV/Vis (CHCl_3): λ_{max} (ϵ) = 285 (106193), 297 (101515), 318 (105301), 341 (sh) (62344), 365 nm (sh) ($20772\text{ M}^{-1}\text{ cm}^{-1}$); UV/Vis (1:2 $\text{CHCl}_3/\text{MeOH}$): λ_{max} (ϵ) = 283 (106907), 294 (103065), 316 (102256), 341 (sh) (57144), 365 nm (sh) ($19345\text{ M}^{-1}\text{ cm}^{-1}$); fluorescence emission ($[3] = 2.92 \times 10^{-6}\text{ mol dm}^{-3}$ in CHCl_3 , 318 nm excitation): $\lambda_{\text{max}} = 400\text{ nm}$; IR: $\tilde{\nu} = 2922\text{ (m)}, 2219\text{ (m)} (\text{C}=\text{C}), 1567\text{ (s)}, 1559\text{ (s)}, 1475\text{ (s)}, 1450\text{ (s)}, 1432\text{ (s)}, 798\text{ (s)}, 757\text{ (s)}, 637\text{ (m)}$; FABMS (10% $\text{CF}_3\text{COOH}/\text{CHCl}_3$): m/z (%): 1208 (100) [$M^+ + \text{H}$]; HRMS (FAB, 10–20% $\text{CF}_3\text{COOH}/\text{CHCl}_3$, [$M^+ + \text{H}$]) calcd for $\text{C}_{90}\text{H}_{43}\text{N}_6$: 1207.3549; found: 1207.3554.

Acknowledgement

The Collège de France is acknowledged for financial support and Roland Graff for the $^1\text{H NMR}$ COSY, NOESY, ROESY and $^1\text{H}-^{13}\text{C}$ HMQC experiments. Dr Bernard Dietrich, Prof. Masakazu Ohkita, Prof. Alexandre Varnek and Dr Jonathan Nitschke are also thanked for helpful discussions.

- [1] *Comprehensive Supramolecular Chemistry, Vol. 10* (Eds.: J.-M. Lehn, J. L. Atwood, J. E. D. Davies, D. D. McNicol, F. Vögtle, D. N. Reinhoudt), Pergamon, Oxford, **1996**.
- [2] a) For reviews on the use of macrocyclic complexes in medical diagnostics, see for example: *Top. Curr. Chem.* **2002**, *221*, whole volume; b) D. Parker in *Comprehensive Supramolecular Chemistry, Vol. 10* (Eds.: J.-M. Lehn, J. L. Atwood, J. E. D. Davies, D. D. McNicol, F. Vögtle, D. N. Reinhoudt), Pergamon, Oxford, **1996**, Chapter 17, pp. 487–536; c) D. Parker, S. R. Cooper in *Crown Compounds: Towards Future Applications* (Ed.: S. R. Cooper), VCH, NY, **1992**, pp. 51–67 and pp. 285–302; d) For the use of macrocycles in drug delivery, see: K.-H. Frömring in *Comprehensive Supramolecular Chemistry, Vol. 10* (Eds.: J.-M. Lehn, J. L. Atwood, J. E. D. Davies, D. D. McNicol, F. Vögtle, D. N. Reinhoudt), Pergamon, Oxford, **1996**, Chapter 16, pp. 445–485.

- [3] E. Blasius, K.-P. Janzen, *Top. Curr. Chem.* **1981**, *98*, 163.
- [4] a) J. D. Lamb, R. G. Smith in *Comprehensive Supramolecular Chemistry, Vol. 10* (Eds.: J.-M. Lehn, J. L. Atwood, J. E. D. Davies, D. D. McNicol, F. Vögtle, D. N. Reinhoudt), Pergamon, Oxford, **1996**, Chapter 4, pp. 79–112; b) L. Echegoyen, R. C. Lawson in *Comprehensive Supramolecular Chemistry, Vol. 10* (Eds.: J.-M. Lehn, J. L. Atwood, J. E. D. Davies, D. D. McNicol, F. Vögtle, D. N. Reinhoudt), Pergamon, Oxford, **1996**, Chapter 6, pp. 151–170; c) Z. Chen, L. Echegoyen in *Crown Compounds: Towards Future Applications* (Ed.: S. R. Cooper), VCH, NY, **1992**, pp. 27–39.
- [5] C. L. Liotta in *Synthetic Multidentate Macrocyclic Compounds* (Eds.: R. M. Izatt, J. J. Christensen), Academic Press, NY, **1978**, pp. 111–205.
- [6] A. Harada, Y. Ederle, K. S. Naraghi, P. J. Lutz in *Materials Science and Technology: A Comprehensive Treatment, Vol. 18* (Eds.: R. W. Cahn, P. Haasen, E. J. Kramer, A.-D. Schlüter), Wiley-VCH, Weinheim, Germany, **1999**, Chapter 14, pp. 485–512; Chapter 19, pp. 621–647.
- [7] H. Hashimoto in *Comprehensive Supramolecular Chemistry, Vol. 3* (Eds.: J. L. Atwood, J. E. D. Davies, D. D. McNicol, F. Vögtle, J. Szejtli, T. Osa), Pergamon, Oxford, **1996**, pp. 483–502.
- [8] E. Mena-Osteritz, P. Bäuerle, *Adv. Mater.* **2001**, *13*, 243.
- [9] F. Vögtle, *Cyclophan-Chemie, Synthesen, Strukturen, Reactionen*, Teubner, Stuttgart, **1990**.
- [10] P. Ruggli, *Justus Liebigs Ann. Chem.* **1912**, *392*, 92.
- [11] H. Meier, *Synthesis* **1972**, 235.
- [12] a) K. G. Utich, D. C. Wysocki, *J. Am. Chem. Soc.* **1966**, *88*, 2608; b) W. H. Okamura, F. Sondheimer, *J. Am. Chem. Soc.* **1967**, *89*, 5991.
- [13] For an informative series of reviews covering the field up to 1999, see: *Top. Curr. Chem.* **1999**, *201*, whole volume.
- [14] *Top. Curr. Chem.* **1999**, *199*, whole volume.
- [15] a) K. M. Merz Jr, R. Hoffmann, A. T. Balaban, *J. Am. Chem. Soc.* **1987**, *109*, 6742; b) R. H. Baughman, H. Eckhardt, M. Kertesz, *J. Chem. Phys.* **1987**, *87*, 6687; c) F. Diederich, Y. Rubin, *Angew. Chem.* **1992**, *104*, 1123; *Angew. Chem. Int. Ed. Engl.* **1992**, *31*, 1101; d) F. Diederich, *Nature* **1994**, *369*, 199; e) P. E. Eaton, E. Galoppini, R. Gilardi, *J. Am. Chem. Soc.* **1994**, *116*, 7588; f) K. S. Feldman, C. K. Weinreb, W. J. Youngs, J. D. Bradshaw, *J. Am. Chem. Soc.* **1994**, *116*, 9019; g) T. Lange, J.-D. van Loon, R. R. Tykwinski, M. Schreiber, F. Diederich, *Synthesis* **1996**, 537.
- [16] J. S. Moore, *Acc. Chem. Res.* **1997**, *30*, 402.
- [17] P. J. Garratt in *Comprehensive Organic Chemistry; The Synthesis and Reactions of Organic Compounds, Vol. 1* (Ed.: J. F. Stoddart), Pergamon, Oxford, **1979**, Chapter 2.6, p. 361.
- [18] a) M. M. Haley, *Synlett* **1998**, 557; b) J. J. Pak, T. J. R. Weakley, M. M. Haley, *J. Am. Chem. Soc.* **1999**, *121*, 8182; c) W. J. Youngs, C. A. Tessier, J. D. Bradshaw, *Chem. Rev.* **1999**, *99*, 3153; d) J. M. Kehoe, J. H. Kiley, J. J. English, C. A. Johnson, R. C. Petersen, M. M. Haley, *Org. Lett.* **2000**, *2*, 969.
- [19] a) A. M. Boldi, F. Diederich, *Angew. Chem.* **1994**, *106*, 482; *Angew. Chem. Int. Ed. Engl.* **1994**, *33*, 468; b) S. Eisler, R. R. Tykwinski, *Angew. Chem.* **1999**, *111*, 2138; *Angew. Chem. Int. Ed. Engl.* **1999**, *38*, 1940.
- [20] a) L. T. Scott, G. J. DeCicco, J. L. Hyun, G. Reinhardt, *J. Am. Chem. Soc.* **1985**, *107*, 6546; b) L. T. Scott, M. J. Cooney, C. Otte, C. Puls, T. Haumann, R. Boese, P. J. Carroll, A. B. Smith III, A. de Meijere, *J. Am. Chem. Soc.* **1994**, *116*, 10275; it may be noted that the name “pericyclines” used in the last two references has been replaced by the name “pericyclines” in the review of reference [13].
- [21] a) A. de Meijere, S. Kozhushkov, C. Puls, T. Haumann, R. Boese, M. J. Cooney, L. T. Scott, *Angew. Chem.* **1994**, *106*, 934; *Angew. Chem. Int. Ed. Engl.* **1994**, *33*, 869; b) A. de Meijere, S. Kozhushkov, T. Haumann, R. Boese, C. Puls, M. J. Cooney, L. T. Scott, *Chem. Eur. J.* **1995**, *1*, 124.
- [22] For porphyrin-incorporated ethynyl cyclophanes, see: a) S. Anderson, H. L. Anderson, J. K. M. Sanders, *Acc. Chem. Res.* **1993**, *26*, 469; b) J. K. M. Sanders in *Comprehensive Supramolecular Chemistry, Vol. 9* (Eds.: J. L. Atwood, J. E. D. Davies, D. D. McNicol, F. Vögtle, J.-P. Sauvage, M. Wais Hosseini), Pergamon, Oxford, **1996**, Chapter 4, p. 131; *para*-phenylethynyl belts: c) T. Kawase, N. Ueda, K. Tanaka, Y. Seirai, M. Oda, *Tetrahedron Lett.* **2001**, 5509; binaphthyl cyclophane receptors: d) U. Neidlein, F. Diederich, *Chem. Commun.* **1996**, 1493;

- acetylenosaccharides: e) R. Bürl, A. Vasella, *Angew. Chem.* **1997**, *109*, 1945; *Angew. Chem. Int. Ed. Engl.* **1997**, *36*, 1852.
- [23] J. Zhang, J. S. Moore, *J. Am. Chem. Soc.* **1994**, *116*, 2655.
- [24] D. Venkataraman, S. Lee, J. Zhang, J. S. Moore, *Nature* **1994**, *371*, 591.
- [25] R. Boese, A. J. Matzger, K. P. C. Vollhardt, *J. Am. Chem. Soc.* **1997**, *119*, 2052.
- [26] For examples of ethynyl macrocycles that externally bind metal ions, see: a) K. Campbell, R. McDonald, N. R. Branda, R. R. Tykwinski, *Org. Lett.* **2001**, *3*, 1045; b) O. Henze, D. Lentz, A. Schäfer, P. Franke, A. D. Schlüter, *Chem. Eur. J.* **2002**, *8*, 357; c) reference [18c].
- [27] a) P. N. W. Baxter, *J. Org. Chem.* **2001**, *66*, 4170; the term "twistophane" is used to describe ethynyl cyclophanes that are completely *ortho*-conjugated, yet helically twisted and, therefore, nonplanar chiral structures. Such molecules represent a small but slowly emergent subclass of conjugated ethynyl macrocycles of which **1**, **2** and **3** are the first reported examples with integrated heterocyclic N-donor sites for metal ion coordination. Examples of this type of molecule include the following: b) M. J. Marsella, Z.-Q. Wang, R. J. Reid, K. Yoon, *Org. Lett.* **2001**, *3*, 885; c) S. K. Collins, G. P. A. Yap, A. G. Fallis, *Org. Lett.* **2000**, *2*, 3189; d) S. K. Collins, G. P. A. Yap, A. G. Fallis, *Angew. Chem. Int. Ed. Engl.* **2000**, *39*, 385; e) M. M. Haley, M. L. Bell, J. J. English, C. A. Johnson, T. J. R. Weakley, *J. Am. Chem. Soc.* **1997**, *119*, 2956; f) K. P. Baldwin, R. S. Simons, J. Rose, P. Zimmerman, D. M. Hercules, C. A. Tessier, W. J. Youngs, *Chem. Commun.* **1994**, 1257; g) reference [18c].
- [28] The construction of ethynyl macrocycles that incorporate pyridine and pyridine-type units has recently attracted a flurry of interest. For examples of conjugated ethynyl macrocycles incorporating pyridine units, see a) Y. Tobe, H. Nakanishi, M. Sonoda, T. Wakabayashi, Y. Achiba, *Chem. Commun.* **1999**, 1625; b) Y. Tobe, A. Nagano, K. Kawabata, M. Sonoda, K. Naemura, *Org. Lett.* **2000**, *2*, 3265; c) S.-S. Sun, A. J. Lees, *Organometallics* **2001**, *20*, 2353; d) reference [26a]; For other examples of conjugated ethynyl macrocycles incorporating bipyridine units, see e) O. Henze, D. Lentz, A. D. Schlüter, *Chem. Eur. J.* **2000**, *6*, 2362; f) reference [26b]; for an example of a conjugated phenylethynyl macrocycle incorporating phenanthroline units, see g) M. Schmittel, H. Ammon, *Synlett* **1999**, 750.
- [29] For the employment of analyte-binding-induced mechanical distortions in linear conjugated polymers as a principle for sensing, see for example: a) D. H. Charych, J. O. Nagy, W. Spevak, M. D. Bednarski, *Science* **1993**, *261*, 585; b) R. D. McCullough, P. C. Ewbank, R. S. Loewe, *J. Am. Chem. Soc.* **1997**, *119*, 633; c) T. M. Swager, *Acc. Chem. Res.* **1998**, *31*, 201; d) S. Okada, S. Peng, W. Spevak, D. Charych, *Acc. Chem. Res.* **1998**, *31*, 229; recent investigations have shown that the twisted and coplanar forms of 1, 4-bis(phenylethynyl)benzene are spectroscopically distinct species, see: e) M. Levitus, K. Schmieder, H. Ricks, K. D. Shimizu, U. H. F. Bunz, M. A. Garcia-Garibay, *J. Am. Chem. Soc.* **2001**, *123*, 4259; the difference originates from the excited state which can exist as energetically different structures, the all-planar one of which has a delocalised cumulene-type bonding pattern. This also supports the expectation that mechanical variations in **2** may be accompanied by spectroscopic changes.
- [30] Reports on the use of pyridine-type ligands connected to/or within electronically delocalised organic scaffolds for the sensing of metal ions are sparse. See for example: a) B. Wang, M. R. Wasielewski, *J. Am. Chem. Soc.* **1997**, *119*, 12; b) M. Kimura, T. Horai, K. Hanabusa, H. Shirai, *Adv. Mater.* **1998**, *10*, 459; c) P. N. W. Baxter, *J. Org. Chem.* **2000**, *65*, 1257; d) D. T. McQuade, A. E. Pullen, T. M. Swager, *Chem. Rev.* **2000**, *100*, 2537; e) C.-S. Choi, T. Mutai, S. Arita, K. Araki, *J. Chem. Soc. Perkin Trans. 2*, **2000**, 243; f) reference [27a].
- [31] K. Sonogashira, Y. Tohda, N. Hagihara, *Tetrahedron Lett.* **1975**, 4467.
- [32] P. Dierkes, P. W. N. M. van Leeuwen, *J. Chem. Soc. Dalton Trans.* **1999**, 1519.
- [33] a) I. R. Butler, C. Soucy-Breau, *Can. J. Chem.* **1991**, *69*, 1117; b) J. Suffert, R. Ziessel, *Tetrahedron Lett.* **1991**, *32*, 757; c) V. Grosshenny, F. M. Romero, R. Ziessel, *J. Org. Chem.* **1997**, *62*, 1491.
- [34] The successful alkylation of 2, 9-dibromo-1, 10-phenanthroline using alkylnylstannanes has been reported, albeit in moderate yields: M. Sjögren, S. Hansson, P.-O. Norrby, B. Åkermark, M. E. Cucciolito, A. Vitagliano, *Organometallics* **1992**, *11*, 3954.
- [35] M. Ohkita, K. Ando, T. Suzuki, T. Tsuji, *J. Org. Chem.* **2000**, *65*, 4385.
- [36] M. Furber in *Comprehensive Organic Functional Group Transformations, Vol. 1* (Eds.: A. R. Katritzky, O. Meth-Cohn, C. W. Rees, S. M. Roberts), Pergamon, Oxford, **1995**, Chapter 1.21, p. 997, and references therein.
- [37] D. O'Krongly, S. R. Denmeade, M. Y. Chiang, R. Breslow, *J. Am. Chem. Soc.* **1985**, *107*, 5544.
- [38] For an example of the use of semiempirical AM1 calculations for successfully predicting the conformations of ethynyl macrocycles, see: M. Srinivasan, S. Sankararaman, H. Hopf, I. Dix, P. G. Jones, *J. Org. Chem.* **2001**, *66*, 4299.
- [39] Further studies on, for example, chirally functionalised derivatives may thus be necessary in order to clarify the solution dynamics of **2**.
- [40] Interestingly, a somewhat higher energy conformational minimum accessible to **3** is that of a triangular tube-type structure. In this conformation, the three bipyridine units are *transoid* and planar, and define the walls of a tubular void. Cyclophane **3** may therefore also be capable of forming inclusion complexes with guests of complementary size and shape to the triangular cavity.
- [41] The metal salts and complexes used in the study were CrCl₃·6H₂O, FeCl₂, CoCl₂·6H₂O, NiCl₂·6H₂O, [PdCl₂(MeCN)₂] and [PtCl₂(MeCN)₂]. All remaining cations investigated were in the form of their anhydrous triflates. The chromium, iron, cobalt and nickel chlorides were each dissolved in a drop of distilled water prior to the preparation of the standard solutions in methanol to ensure complete solubility. For the same reason, the palladium and platinum complexes were initially dissolved in warm acetonitrile (1 mL). The Cu^{II}, Ag^I, Hg^{II} and Tl^I triflates used were >>99.9% purity.
- [42] The requirement of 1.5 equivalents of Ag^I for complete coordination of **3** rather than the expected 1:1 **3**/Ag^I ratio, suggests a concentration-dependent binding process. This indicates that a relatively weak association between **3** and Ag^I exists at low [3].
- [43] For a study of π-cation interactions between benzenoid cyclophanes and Hg^{II}, Tl^I and Ag^I, see: a) J. Gross, G. Harder, A. Siepen, J. Harren, F. Vögtle, H. Stephan, K. Gloe, B. Ahlers, K. Cammann, K. Rissanen, *Chem. Eur. J.* **1996**, *2*, 1585; b) For complexes possessing ethyne-HgX₂ interactions, see: W. Frosch, A. del Villar, H. Lang, *J. Organomet. Chem.* **2000**, *602*, 91. For ethyne-PdR₂ interactions, see: c) R. Usón, J. Forniés, M. Tomás, B. Menjón, A. J. Welch, *J. Organomet. Chem.* **1986**, *304*, C24.
- [44] Cu^{II} is a significant environmental pollutant and an essential trace element of life. Copper proteins occur in bacteria, plants, higher organisms and mammals and perform many diverse functions. For example, superoxide dismutase removes the toxic superoxide radical anion produced by phagocytes, cytochrome c oxidase mediates the last phosphorylation in the respiratory chain, the monooxygenases dopamine β-monooxygenase and tyrosinase perform catalytic oxidative transformations in the adrenal cortex and skin respectively, plastocyanin and azurin participate in plant and bacterial photosynthesis, and ceruloplasmin mediates copper transport and storage. In view of the manifold biological roles of copper, the discovery of new lead sensors for this important element will continue to be of especial interest. For recent examples of fluorescence chemosensors for Cu^{II} ions, see: a) F. Pina, M. A. Bernardo, E. García-España, *Eur. J. Inorg. Chem.* **2000**, 2143; b) Y. Zheng, Q. Huo, P. Kele, F. M. Andreopoulos, S. M. Pham, R. M. Leblanc, *Org. Lett.* **2001**, *3*, 3277; c) M. Beltramello, M. Gatos, F. Mancin, P. Tecilla, U. Tonellato, *Tetrahedron Lett.* **2001**, *42*, 9143.
- [45] Within the context of the above work, the qualitative parameters used to describe the metal-ion binding and sensing properties of ligands **2**, **3** and **9**, are defined as follows: *Complexation selectivity*, that is, the number of different types of metal ions that a given ligand is able to complex; the greater the number, the lower the selectivity. *Complexation discrimination*, that is, the number of strongest coordinating metal ions that equally bind to a given ligand; the higher the number, the less the discrimination. *Sensory selectivity*, the number of coordinating metal ions that produce similar fluorescence responses; the higher the number, the less the fluorescence selectivity. *Output signal intensity*, the estimated fluorescence detection limit for a given metal ion, which may be signalled both visually and instrumentally.
- [46] The fluorescence emission detection limits for Ag^I by **2** and Cu^{II} by **3** were estimated to be at [Ag^I]=1×10⁻⁶ and [Cu^{II}]=6×10⁻⁷ mol dm⁻³, respectively, whereas the estimated detection limit

for Zn^{II} by **1** was at $[Zn^{II}] = 3 \times 10^{-6} \text{ mol dm}^{-3}$ in 1:2 $CHCl_3/MeOH$. The fluorescence responses of **2** and **3** appear to be generally slightly more sensitive to the presence of metal ions than that of **1**. However, if complexation-induced mechano-structural changes are occurring in **2** and **3**, the resulting influence upon fluorescence signal amplification must be small. The above results suggest that increasing the conjugation and electronic delocalisation of the sensors may be a more effective future approach to optimising the fluorescence emission sensitivity and thus lowering the sensory detection limit for particular metal ions.

[47] Molecules **2**, **3** and **9** may be regarded as members of a lead class of metal sensors, as they are structurally significantly different from systems normally employed for this purpose. In particular, **2** and **3** are among the first examples of the utilisation of conjugated cyclic ethynyl

scaffolds for metal-ion sensory applications. The majority of traditional ion sensors are constructed from nonaromatic cyclic and acyclic binding sites connected to or incorporated into classical fluorophores such as fluorescein. See for example, K. R. Gee, Z.-L. Zhou, W.-J. Qian, R. Kennedy, *J. Am. Chem. Soc.* **2002**, *124*, 776.

- [48] D. R. Coulson, L. C. Satek, S. O. Grim, *Inorg. Synth.* **1990**, *28*, 107.
[49] J. S. Brumbaugh, A. Sen, *J. Am. Chem. Soc.* **1988**, *110*, 803.
[50] B. Corain, B. Longato, G. Favero, D. Ajò, G. Pilloni, U. Russo, F. R. Kreissl, *Inorg. Chim. Acta.* **1989**, *157*, 259.
[51] J. E. Parks, B. E. Wagner, R. H. Holm, *J. Organomet. Chem.* **1973**, *56*, 53.

Received: May 15, 2002 [F4095]